ELSEVIER

Surface Science Reports 32 (1998) 291–340

surface science reports

Reactions at surfaces studied by ab initio dynamics calculations

Axel Groß*,[1]

Fritz-Haber-Institut der Max-Planck-Gesellschaft, Faradayweg 4–6, D-14195 Berlin-Dahlem, Germany

Manuscript received in final form 30 June 1998

Abstract

Owing to the development of efficient algorithms and the improvement of computer power it is now possible to map out potential energy surfaces (PESs) of reactions at surfaces in great detail. This achievement has been accompanied by an increased effort in the dynamical simulation of processes on surfaces. The paradigm for simple reactions at surfaces – the dissociation of hydrogen on metal surfaces – can now be treated fully quantum dynamically in the molecular degrees of freedom from first principles, i.e., without invoking any adjustable parameters. This relatively new field of ab initio dynamics simulations of reactions at surfaces will be reviewed. Mainly the dissociation of hydrogen on clean and adsorbate covered metal surfaces and on semiconductor surfaces will be discussed. In addition, the ab initio molecular dynamics treatment of reactions of hydrogen *atoms* with hydrogen-passivated semiconductor surfaces and recent achievements in the ab initio description of laser-induced desorption and further developments will be addressed.

1. Introduction

Understanding reactions on surfaces plays an important role in a wide range of technologically relevant applications. Among those are the *heterogenous catalysis* – the majority of reactions in the chemical industry employ catalysts; *crystal growth*, which determines, e.g., the quality of semiconductor devices; *corrosion* and *lubrication*, which influences the durability of mechanical systems; or *hydrogen storage* in metals, just to mention a few. The reactions involved in these processes are often too complicated to be studied in detail as a whole. Therefore in surface science one tries to understand reaction mechanisms by breaking them up into simpler steps which are then studied under well-defined conditions [1,2].

Studies of chemical reaction dynamics are well established in the gas phase. Reactions on surfaces differ from gas-phase reactions in two fundamental aspects: first, the presence of the surface changes the symmetry significantly, and second, the substrate on which the reaction occurs represents in principle a system with an infinite number of degrees of freedom which acts as a heat bath that leads to dissipation and thermal fluctuations. As for the symmetry, while for example for the description of the

* Tel.: +49-30-8413-4818; fax: +49-30-8413-4701; e-mail: gross@fhi-berlin.mpg.de

[1] New address: Physik-Department T30, Technische Universität München, D-85747 Garching, Germany.

0167-5729/98/$ – see front matter
PII: S0167-5729(98)00008-9

dissociation of a diatomic molecule in the gas phase only the interatomic distance has to be taken into account (all other degrees of freedom can be separated), in front of a surface all six degrees of freedom of the diatomic molecule have to be considered explicitly since the surface breaks the symmetry with respect to the gas phase. On the other hand, a crystalline surface introduces new symmetries, for example the periodicity of the surface.

Dissociative adsorption processes are of particular importance for reactions on surfaces since they constitute the first step in heterogenous catalysis; furthermore they are often the rate-limiting process, for example in ammonia synthesis or CO oxidation. The term "heterogeneous" refers to the fact that the reactants (usually a gas) and the catalyst (usually a solid substrate) are not in the same phase state. For the atomic or molecular adsorption process, energy dissipation to the substrate is necessary for the particles to be trapped into an adsorption well on the surface, otherwise they would be scattered back into the gas phase. In the case of dissociative adsorption, however, there is another channel for energy transfer, which is the conversion of the kinetic and internal energy of the molecule into translational energy of the atomic fragments on the surface relative to each other. In addition, for light molecules like hydrogen there is usually only a small energy transfer to substrate phonons due to the large mass mismatch between the molecule and the substrate atoms. If furthermore no substantial surface rearrangement upon adsorption occurs – which is often fulfilled for densely packed metal surfaces – then the dissociative adsorption dynamics can be described using low-dimensional potential energy surfaces (PESs).

Still the interaction of a diatomic molecule with a well-defined fixed substrate involves the six degrees of freedom of the molecule. Up to recently the interaction dynamics in particular of hydrogen had been described in low-dimensional quantum studies [3–27]; higher-dimensional studies could only be performed by classical trajectory calculations [28–30] or mixed quantum-classical methods [31–34] on model potentials. This was due to the lack of reliable potential energy surfaces and the large computational effort for high-dimensional quantum dynamics studies (for reviews on these dynamical studies see, e.g., [35–38]). This situation has changed significantly within the last five years caused by the development of efficient algorithms and the increase in computer power. For the paradigm of simple reactions on surfaces – the dissociation of hydrogen on metal surfaces – detailed potential energy surfaces obtained by density functional theory calculations are now available [39–49]. This has increased the motivation to perform dynamical studies in which all hydrogen degrees of freedom are treated explicitly, and indeed the first six-dimensional quantum dynamical studies of hydrogen dissociation on metal surfaces have now been performed [50–53].

In this review I will give an overview of this rather new field of ab initio dynamics calculations of reactions on surfaces. Usually these calculations require three independent steps:

1. determination of the ab initio PES by first-principles total-energy calculations,
2. a fit of the total energies to an analytical or numerical continuous representation which serves as an interpolation between the actually calculated points,
3. a dynamical calculation on this representation of the ab initio PES that includes all relevant degrees of freedom.

Since this type of calculations is indeed derived from first principles with no adjustable parameters, I will refer to them as "ab initio dynamics calculations". However, this term should not conceal the still approximative nature of these dynamics simulations. In all three steps approximations are involved which will be discussed in this review. For example, exchange and correlation effects of the electrons

cannot be treated exactly in total-energy calculations using density functional theory. The description of the surface by either a supercell or a cluster method is an approximation. Furthermore, the fitting of the ab initio energies to a continuous representation is a highly non-trivial task. If just classical trajectories are determined, quantum effects in the motion of the nuclei are neglected which can be important, in particular for the dynamics of hydrogen. Also the question, what are the relevant degrees of freedom in the dissociation process, cannot be answered unambiguously and depends, for example, on the properties that one is interested in. Hence in this review also investigations, in which not all molecular degrees of freedom are treated explicitly, but which are still derived from first principles, are included.

For classical ab initio dynamics simulations, which will in the following be referred to by the term "ab initio molecular dynamics", the three steps mentioned above can actually be combined since most first-principles total-energy schemes also determine the gradients of the potential via the Hellmann–Feynman theorem [54,55]. Thus the classical equations of motion can be directly solved. For each step of the numerical integration of the equations of motion the forces are determined by a new total-energy calculation. Since this is rather time-consuming, only a small number ($\lesssim 100$) of trajectories can be calculated in this way. Therefore this method does not allow the determination of reaction probabilities which usually require at least thousands of trajectories due to the statistical nature of the reactive events [51].

On the other hand, ab initio molecular dynamics simulations with the determination of the forces "on the fly" do not require any fitting. This makes them very flexible. On semiconductor surfaces, the substrate rearrangement upon adsorption cannot be neglected; indeed it plays a crucial role for the adsorption and desorption mechanism [9,56]. An analytical fit of an ab initio PES including several substrate degrees of freedom has not been performed yet because of its complexity. Therefore, for the investigation of the dissociative adsorption and associative desorption process on semiconductor surfaces the "traditional" ab initio molecular dynamics method with the determination of the forces "on the fly" has still been used [57–60]. Its application is reasonable if the information obtained from a small number of trajectories is sufficient to gain insight into a particular process.

High-dimensional ab initio dynamics calculations will not make low-dimensional simulations on model potentials obsolete. These model calculations have provided us with the framework to interprete the dynamics. High-dimensional dynamics is often too complicated to be followed in detail. But this review will show that high-dimensional ab initio dynamics calculations have advanced our understanding of the dissociation dynamics tremendously and sometimes even caused the modification of established concepts. First of all, the ab initio calculation of potential energy surfaces has confronted the gas–surface dynamics community with some features of these PESs which had not been expected and which challenged new interpretations and calculations. And secondly, some phenomema in the reaction dynamics on surfaces only occur in simulations if a sufficiently large number of degrees of freedom is included. Thus high-dimensional simulations not only lead to progress in the quantitative, but also in the qualitative understanding of processes on surfaces. In particular for the hydrogen dissociation on transition metal surfaces ab initio dynamics calculations have proven their power. They demonstrated, e.g., that the initial decrease of the sticking probability with kinetic energy often found experimentally in these systems is not due to a precursor mechanism, as was the common believe, but is caused by a hitherto underestimated dynamical mechanism, namely the steering effect [52,61].

This review is devoted to a large part to the dissociation of hydrogen on surfaces. From the theoretical point of view, hydrogen is the simplest molecule. This does not neccessarily keep the computational effort small, but it makes the theoretical description controllable. From the experimental

point of view, hydrogen molecules can be used without severe problems in molecular beam apparatuses, and they can be detected state-specifically by laser techniques. Therefore hydrogen is the ideal candidate for a close collaboration between theory and experiment in order to explore the dynamics of the dissociation process on surfaces. The general concepts found in these studies will also be applicable to heavier and more complicated molecules. Due to its light mass, the study of the hydrogen dissociation dynamics also allows us to address some fundamental concepts in physics like the importance of quantum effects. Still the hydrogen interaction with surface is technologically relevant, for example in the passivation or growth of semiconductor devices. All these facts make the study of the hydrogen dissociation dynamics on surfaces an exciting research subject.

The electronically adiabatic ab initio dynamics of adsorption and desorption has recently been reviewed from a more quantum chemical point of view [60]. In the meantime, an ab initio molecular dynamics study of the reaction of hydrogen *atoms* with a hydrogen-passivated semiconductor surface has been performed [62] in which pick up reactions of the Eley–Rideal type were studied. Furthermore, detailed ab initio PES studies of reactions on surfaces involving heavier molecules like O_2 [63–65] or CO_2 [66,67] have been performed, and probably soon dynamics calculations using these ab initio potentials will be carried out. Even the laser-induced desorption which involves electronically excited states has currently been addressed from first principles, namely the laser-induced desorption of NO from NiO(1 0 0) [68,69], which will also be briefly reviewed at the end of this article. This short collection shows that ab initio dynamics studies of reactions on surface is a very active and growing field.

After this introduction, in the next section the theoretical concepts necessary in order to perform ab initio dynamics calculations are briefly introduced. Then the hydrogen dissociation on metal surfaces is addressed, first on simple and noble metals where the dissociation is usually hindered by a substantial barrier, and then on transition metals which often have non-activated pathways to dissociative adsorption. In this context also the poisoning of the dissociation by an adsorbate is discussed. The interaction of hydrogen with semiconductor surfaces is treated in the following section. Then the first ab initio dynamics calculation involving electronically excited states is discussed. The review ends with an outlook and some concluding remarks.

2. Theoretical background

In this section the theoretical methods to describe the molecule–surface interaction are briefly described. It is not intended to give a complete overview. I will rather introduce the main concepts and shortly comment on them.

2.1. Born–Oppenheimer approximation

The Schrödinger equation describing the interaction of molecules with surfaces has the general form

$$\mathcal{H} \mid \Psi(\{\mathbf{R}_m, \mathbf{r}_n\})\rangle = \mathcal{E} \mid \Psi(\{\mathbf{R}_m, \mathbf{r}_n\})\rangle. \tag{1}$$

In this equation $\mathbf{R}_m$ are the ionic coordinates and $\mathbf{r}_n$ the electronic coordinates. It is well known that a complete analytical solution of the Schrödinger equation taking into account both ionic and electronic degrees of freedom is not possible except for simple cases. One common approach is to assume that –

due to the large mass difference between electrons and the nuclei – the electrons follow the motion of the nuclei adiabatically. This is the famous Born–Oppenheimer approximation [70]. Since it is only an approximation, its validity has to be checked carefully.

In gas-surface scattering electronically non-adiabatic processes are indeed occurring. They are directly observable as chemiluminescence and exo-electron emission (see, e.g., the recent review of Greber [71]). However, the proper treatment of electronically non-adiababic effects in gas-surface dynamics is rather complex. One problem that goes with the complexity of the non-adiabaticity is that it is not easy to judge whether the dynamics in any particular system is indeed electronically adiabatic or not. The usual argument for the validity of the Born–Oppenheimer approximation is the smallness of the atomic velocities as compared to the electronic velocities. If in addition the adiabatic energy levels are well-separated, electronic transitions are negligible (see, e.g., [72]). For metals the situation is more complicated due to the quasi-continuum of electronic states. Since the effective potentials and the coupling between the electronic states can still not be computed rigorously, one is left with more or less hand-waving arguments. Among them are the following: (i) At metal surfaces electronic excitations are very short-lived. Hence electronic excitations are effectively quenched. (ii) Molecular electronic levels become rather broad upon the interaction with surfaces. Broad levels correspond to short lifetimes of excited states and again, this leads to an effective quenching of electronic excitations.

On semiconductor and insulator surfaces the situation is different due to the band gap which makes the treatment of electronically excited states more tractable. At the end of this review I will present the first description of electronically non-adiabatic processes in molecular desorption from oxide surfaces on an ab initio basis. For metal surfaces, where no band gap exists, a more practical approach has still to be applied which is just to perform electronically adiabatic dynamical studies of reactions on surfaces as well and detailed as possible and to compare the results of these high-quality calculations with experiment. As long as the consequences of these simulations are in agreement with experiment, there is apparently no need for the involvement of electronic excitations in the described processes. For the time being, we just follow this practical approach and assume that the Born–Oppenheimer approximation is justified. We can then write down the electronic Hamiltonian in which the coordinates of the nuclei just enter as parameters. This Hamiltonian has the form

$$H_{\mathrm{el}}\left(\{\mathbf{R}_m\}\right)\,|\psi(\{\mathbf{r}_n\})\rangle \;=\; E\left(\{\mathbf{R}_m\}\right)\,|\psi(\{\mathbf{r}_n\})\rangle. \tag{2}$$

The many-electron ground state energy $E_0(\{\mathbf{R}_m\})$ then defines the potential for the motion of the nuclei. Once it is obtained, it can be plugged into the Schrödinger equation for the nuclei,

$$\left(\sum_i \frac{-\hbar^2}{2M_i}\nabla^2_{\mathbf{R}_i} \;+\; E_0(\{\mathbf{R}_m\})\right)\,\Phi(\{\mathbf{R}_m\}) = \;\mathcal{E}\,\Phi(\{\mathbf{R}_m\}), \tag{3}$$

where $\mathcal{E}$ is now the energy relevant for the dynamics of the nuclei, or, alternatively, it can be used to solve the classical equations of motion,

$$M_i\,\frac{\partial^2}{\partial t^2}\mathbf{R}_i \;=\; -\frac{\partial}{\partial \mathbf{R}_i}E_0(\{\mathbf{R}_m\}). \tag{4}$$

For extended systems the most efficient approach to determine the many-electron ground state energy $E_0(\{\mathbf{R}_m\})$ from first principles is density functional theory [73,74] in combination with the supercell concept. In this approach the surface is modelled by a periodic array of slabs separated by vacuum

regions, and the wave functions are expanded in a suitable basis which is often based on plane waves or augmented plane waves. Almost all of the ab initio potentials discussed later in this review are determined in this way, but real-space [75,76] and Green function methods [77–79] have been proposed as well. Also quantum chemical methods are used in which the infinite substrate is modelled by a finite cluster (see, e.g., the recent review of Whitten and Yang [80]). Ab initio total energy calculations are briefly discussed in the next section.

2.2. *Ab initio total energy calculations*

In this review I will focus on the *reaction dynamics on ab initio potential energy surfaces*, not on the determination of the PESs. Still I will introduce some basics about density functional theory (DFT). For further details I refer to more extensive treatments like, e.g., [81,82]. DFT is based upon the Hohenberg–Kohn theorem [73] which states that the ground-state total energy of a system of interacting electrons E_{tot} can be obtained by minimizing an energy functional $E[n]$,

$$E_{\mathrm{tot}} = \min E[n] = \min(T[n] + U[n] + E^{\mathrm{xc}}[n]). \tag{5}$$

$T[n]$ and $U[n]$ are the functionals of the non-interacting many electron kinetic and electrostatic energy, respectively. All quantum mechanical many-body effects are contained in the so far unknown exchange–correlation functional $E^{\mathrm{xc}}[n]$. The electron density $n(\mathbf{r})$ which minimizes the total energy can be found by solving self-consistently the Kohn–Sham equations [74]

$$H\psi_i(\mathbf{r}) = \left[\frac{-\hbar^2}{2m}\nabla^2 + V^{\mathrm{es}}(\mathbf{r}) + V^{\mathrm{xc}}(\mathbf{r})\right]\psi_i(\mathbf{r}) = \varepsilon_i\psi_i(\mathbf{r}), \tag{6}$$

where T is the single-particle kinetic energy operator and $V^{\mathrm{es}}(\mathbf{r})$ the electrostatic potential. The exchange–correlation potential $V^{\mathrm{xc}}(\mathbf{r})$ is the functional derivative of the exchange–correlation functional $E^{\mathrm{xc}}[n]$:

$$V^{\mathrm{xc}}(\mathbf{r}) = \frac{\delta E^{\mathrm{xc}}[n]}{\delta n}. \tag{7}$$

The exchange–correlation functional $E^{\mathrm{xc}}[n]$ can be written as

$$E^{\mathrm{xc}}[n] = \int \mathrm{d}^3\mathbf{r}\; n(\mathbf{r})\; \epsilon^{\mathrm{xc}}[n](\mathbf{r}), \tag{8}$$

where $\epsilon^{\mathrm{xc}}[n]$ is the exchange–correlation energy per particle. This exchange–correlation energy is not known exactly except for some special cases like constant electron density. In a wide range of bulk and surface problems the so-called local density approximation (LDA), in which $\epsilon^{\mathrm{xc}}[n]$ is replaced by the exchange–correlation energy for the homogeneous electron gas, has been surprisingly successful [82]. For dissociation barriers on surfaces, however, LDA is seriously in error. In the generalized gradient approximation (GGA) also the gradient of the density is included in the exchange–correlation functional. Different forms for the GGA functional have been proposed (see, e.g., [83–86]). The use of GGA functionals leads to a significant improvement in the accuracy of calculated barrier heights [39, 85]. Still the validity of the GGA is strongly debated, in particular in the H_2/Si(1 0 0) system [87]. The problem in the development of more accurate exchange–correlation functionals is that they still represent in principle an uncontrolled approximation, i.e., there is no systematic way of improving the

functionals since there is no expansion in some controllable parameter (it should be noted here that even if an expansion in some controllable parameter exists, this expansion can still be problematic). Basically the success justifies the choice of some particular functional. Hence dynamical simulations on ab initio potentials also serve the purpose to check the accuracy of the chosen exchange–correlation functional.

The supercell approach allows one to transfer DFT algorithms, that have been very successfully applied to the determination of bulk properties, to the description of surface problems. Especially the seminal paper by Car and Parrinello [88] has drawn a lot of attention. Due to the variational principle of density functional theory the determination of the electronic ground state can be regarded as a global optimization scheme thus avoiding the explicit diagonalization of huge matrices. Such an approach was first proposed by Bendt and Zunger [89]. Car and Parrinello demonstrated how powerful this method can be by combining DFT and molecular dynamics.

In the quantum chemical approach the infinite substrate is represented by a finite cluster. DFT methods have also been used to determine the total energies of the cluster [90,91], but traditionally quantum chemical methods based on the wave function dominate, i.e. Hartree–Fock methods without or with the inclusion of the configuration interaction (CI). While supercell calculations often describe relatively high-coverage situations due to the repeated surface unit cell, cluster methods represent low-coverage situations. However, they suffer from the fact that the infinite substrate is often not appropriately modelled by a small cluster and that the total energies are often not converged as a function of the cluster size [80]. For the treatment of electronic excitations, DFT methods could in principle also be used because due to the Hohenberg–Kohn theorem the electronic ground state density uniquely defines the external potential [73] and thereby also all electronically excited states. However, in practice DFT methods usually only determine the total energy for the electronic ground state of a certain configuration (there are exceptions, for example see [92]). To describe electronically excited states wave-function based methods are still unavoidable which necessitates the use of a finite cluster that can, however, be embedded for example in a field of point charges [68,69].

2.3. Parametrization of the ab initio potential

One serious problem arises for the use of ab initio potential energies in particular in quantum dynamics simulations. To solve the Schrödinger equation, one needs in general a continuous description of the potential since the wave functions are delocalized. The ab initio calculations, however, just provide total energies for discrete configurations of the nuclei. In order to obtain a continuous description, the ab initio energies have to be fitted to an analytical or numerical continuous representation of the potential energy surface. This is a highly non-trivial task. On the one hand the representation should be flexible enough to accurately reproduce the ab initio input data, on the other hand it should have a limited number of parameters so that it is still controllable. Ideally a good parametrization should not only accurately interpolate between the actually calculated points, but it should also give a reliable extrapolation to regions of the potential energy surface that have actually not been determined by the ab initio calculations.

The explicit form of the chosen analytical or numerical representation of the ab initio potential varies from application to application. Often the choice is dictated by the dynamics algorithm in which the representation is used. The applications have almost entirely been devoted to the interaction of a diatomic molecule with the surface. The angular orientation of the molecule has usually been expanded

in spherical harmonics and the center-of-mass coordinates parallel to the surface in a Fourier series [47, 50,61,93]. For the PES in the plane of the molecular distance from the surface and the interatomic separation a representation in reaction path coordinate has been employed [50,61,93,94], but also two-body potentials have been used [47]. Before detailed ab initio potentials became available, the LEPS form was often used to construct a global PES [35]. This parametrization contains only a small number of adjustable parameters which made it so attractive for model calculations, but which makes it at the same time relatively unflexible. A modified LEPS potential has still been successfully used to fit an ab initio PES of the interaction of atomic hydrogen with the hydrogenated Si(1 0 0) surface [62].

As an alternative approach to fit ab initio energies, a genetic programming scheme has recently been proposed, in which both the best functional form and the best set of parameters are searched for [95]. This method has so far only been used for three-dimensional potentials so that its capability still has to be proven for higher-dimensional problems.

Ab initio total energies are often mainly determined at high-symmetry points of the surface in order to reduce the computational cost. It is true that these high-symmetry points usually reflect the extrema in the PES. However, due to this limitation the fitted continuous PES can only contain terms that correspond to these high-symmetry situations. On the one hand this often saves computer time also in the quantum dynamics because certain additional selection rules are introduced which reduces the necessary basis set [47,50]. On the other hand, of course this represents an approximation. The question, how serious the neglect of terms with lower symmetry is, remains open until these terms have been determined and included in actual dynamical calculations.

If more than just the molecular degrees of freedom should be considered in a parametrization of an ab initio PES, analytical forms become very complicated and cumbersome. As an alternative, the interpolation of ab initio points by a neural network has been proposed [96–98]. Neural networks can fit, in principle, any real-valued, continuous function to any desired accuracy. They require no assumptions of the functional form of the underlying problem. On the other hand, there is no physical insight that is used as an input in this parametrization. Hence the parameters of the neural network do not reflect any physical or chemical property. Another approach is to fit the parameters of a tight-binding formalism to ab initio energies [99]. A tight-binding method is more time-consuming than an analytical representation or a neural network since it requires the diagonalization of a matrix. However, due to the fact that the quantum mechanical nature of bonding is taken into account [1 0 0] tight-binding schemes need a smaller number of ab initio input points to perform a good interpolation *and* extrapolation [101]. In addition, their parameters, the Slater–Koster integrals [102], have a physical meaning. It remains to be seen how useful the different fitting methods will be for performing ab initio dynamics simulations.

It has been argued that any fitting scheme using analytic potential functions introduces a possible bias into the parametrization [60]. In order to avoid this one should use ab initio molecular dynamics methods that calculate the forces "on the fly" because this requires no fitting. However, approaching a problem apparently unbiased also means not to take advantage of any previous knowledge. On the contrary, using as much experience and knowledge as possible should usually make any method more efficient [95].

An important issue is to judge the quality of the fit to an ab initio PES. Usually the root mean squared (RMS) error between fit and input data is used as a measure of the quality of a fit. If this error is zero, then everything is fine. However, normally this error is larger than zero. The systematic error of the ab initio energies is usually estimated to be of the order of 0.1 eV. Often it is said that the RMS error of the

fit should be of the same order. But the dynamics of molecular dissociation at surfaces can be dramatically different depending on whether there is a barrier for dissociation of height 0.1 eV or not [103]. Hence for certain regions of the PES the error has to be much less than 0.1 eV, while for other regions even an error of 0.5 eV might not influence the dynamics significantly. Another example occurs in a reaction path parametrization. If the curvature in the parametrization is off by a few percent, the energetic distribution of barrier heights is not changed and the dynamical properties are usually not altered significantly. However, the location of the barriers is changed and consequently the RMS error can become rather large. Hence one has to be cautious by just using the RMS error as a quality check of the fit. Unfortunately there is no other simple error function for the assessment of the quality of a fit. If it is possible, one should perform a dynamical check. Obviously, if the dynamical properties calculated on a fitted PES agree with the ones calculated on the original PES, the quality of the fit should be sufficient.

2.4. Quantum dynamics

There are two ways to determine quantum mechanical reaction probabilities: by solving the time-dependent or the time-independent Schrödinger equation. Both approaches are equivalent [104] and should give the same results. The chosen method depends on its applicability, but apparently it is often also a matter of training and personal taste.

In the most common time-independent formulation, the concept of defining one specific reaction path coordinate is crucial. Starting from the Schrödinger equation

$$(H - E)\ \Psi = 0, \tag{9}$$

one chooses one specific reaction path coordinate s and separates the kinetic energy operator in this coordinate

$$\left(\frac{-\hbar^2}{2\mu}\partial_s^2 + \tilde{H} - E\right)\ \Psi = 0. \tag{10}$$

Here $\tilde{H}$ is the original Hamiltonian except for the kinetic energy operator in the reaction path coordinate. Usually the use of curvelinear reaction path coordinates results in a more complicated expression for the kinetic energy operator involving cross terms [105–107], but for the sake of clarity I have neglected this in Eq. (10). As the next step one expands the wave function in the coordinates perpendicular to the reaction path coordinate in some suitable set of basis functions,

$$\Psi = \Psi(s, \ldots) = \sum_n \psi_n(s)\ |n\rangle. \tag{11}$$

Here n is a multi-index, and the expansion coefficients $\psi_n(s)$ are assumed to be a function of the reaction path coordinate. Now we insert the expansion of Ψ in Eq. (10) and multiply the Schrödinger equation by $\langle m|$, which corresponds to performing a multi-dimensional integral. Since the basis functions $|n\rangle$ are assumed to be independent of s, we end up with the so-called coupled-channel equations,

$$\sum_n \left\{\left(\frac{-\hbar^2}{2\mu}\partial_s^2 - E\right)\delta_{m,n} + \langle m|\tilde{H}|n\rangle\right\}\psi_n(s) = 0. \tag{12}$$

Instead of a partial differential equation – the original time-independent Schrödinger equation Eq. (9) – we now have a set of coupled ordinary differential equation. Still a straightforward numerical integration of the coupled-channel equations leads to instabilities, except for in simple cases, due to exponentially increasing so-called closed channels. Recently a very stable and efficient coupled-channel algorithm has been introduced [108–111]. The main idea underlying this particular algorithm will be briefly sketched in the following.

For the solution Ψ defined in Eq. (11), which represents a vector in the space of the basis functions, the initial conditions are not specified. This function can also be considered as a matrix

$$\Psi = (\psi)_{nl}, \tag{13}$$

where the index l labels a solution of the Schrödinger equation with an incident plane wave of amplitude one in channel l and zero in all other channels. Formally one can then write the solution of the Schrödinger equation for a scattering problem in a matrix notation as

$$\Psi(s \to +\infty) = \mathrm{e}^{-\mathrm{i}qs} - \mathrm{e}^{\mathrm{i}qs}\, r, \qquad \Psi(s \to -\infty) = \mathrm{e}^{-\mathrm{i}qs}\, t. \tag{14}$$

Here $q = q_m \delta_{m,n}$ is a diagonal matrix, r and t are the reflection and transmission matrix, respectively. Now one makes the following ansatz for the wave function:

$$\Psi(s) = (1 - \rho(s))\, \frac{1}{\tau(s)}\, t. \tag{15}$$

Eq. (15) defines the *local reflection matrix* $\rho(s)$ (LORE) and the *inverse local transmission matrix* $\tau(s)$ (INTRA). The boundary values for these matrices are (except for phase factors which, however, do not affect the transition probabilities):

$$(\rho(s); \tau(s)) = \begin{cases} (r; t) & s \to +\infty, \\ (0; 1) & s \to -\infty. \end{cases} \tag{16}$$

From the Schrödinger equation first-order differential equations for both matrices can be derived [108–111] which can be solved by starting from the known initial values at $s \to -\infty$; at $s \to +\infty$ one then obtains the physical reflection and transmission matrices. Thus the numerically unstable boundary value problem has been transformed to a stable initial value problem.

In the time-dependent or wave-packet formulation, the solution of the time-dependent Schrödinger equation

$$\mathrm{i}\hbar\, \frac{\partial}{\partial t}\, \Psi(\mathbf{R}, t) = H \Psi(\mathbf{R}, t) \tag{17}$$

can formally be written as

$$\Psi(\mathbf{R}, t) = \mathrm{e}^{-\mathrm{i}Ht/\hbar}\, \Psi(\mathbf{R}, t = 0), \tag{18}$$

if the potential is time-independent. The most common methods to represent the time-evolution operator $\exp(-\mathrm{i}Ht/\hbar)$ in the gas–surface dynamics community are the split-operator [112,113] and the Chebychev [114] methods. In the split-operator method, the time-evolution operator for small time steps Δt is written as

$$\mathrm{e}^{-\mathrm{i}H\Delta t/\hbar} = \mathrm{e}^{-\mathrm{i}K\Delta t/2\hbar}\, \mathrm{e}^{-\mathrm{i}V\Delta t/\hbar}\, \mathrm{e}^{-\mathrm{i}K\Delta t/2\hbar} + \mathrm{O}(\Delta t^3), \tag{19}$$

where K is the kinetic energy operator and V the potential term. In the Chebyshev method, the time-evolution operator is expanded as

$$e^{-iH\Delta t/\hbar} = \sum_{j=1}^{j_{max}} a_j(\Delta t)\, T_j(\bar{H}), \tag{20}$$

where the T_j are Chebyshev polynomials and $\bar{H}$ is the Hamiltonian rescaled to have eigenvalues in the range $(-1, 1)$. Both propagation schemes use the fact that the kinetic energy operator is diagonal in **k**-space and the potential in real-space. The wave function and the potential are represented on a numerical grid, and the switching between the **k**-space and real-space representations is efficiently done by fast Fourier transformations (FFT) [115].

In the last years the time-dependent wave-packet methods have been much more fashionable than time-independent schemes in the gas-surface dynamics community. Many different groups have used wave-packet codes to study the dissociation dynamics on surfaces, up to recently almost entirely on low-dimensional model potentials [3–5,10,13,14,16,116–118]. It has been argued that wave-packet methods avoid "the problem of excessively many channels" [38]. But actually these methods suffer from the fact that the wave function and the potential are represented on a grid which leads to memory problems in the implementation. In each dimension between 16 and several hundred grid-points are used. In time-independent methods, on the contrary, it is for example sufficient to expand the hydrogen wave function in the interatomic distance in three or four eigenfunctions of a harmonic oscillator due to the large vibrational energy quantum. One might say that the hydrogen vibration in time-independent methods is represented by three or four points instead of more than 16 in time-dependent methods. In addition, while in the LORE–INTRA scheme [108–111] the matrices are successively determined along the reaction path and do not have to be stored, in wave-packet methods the wave function has always to be stored everywhere on the grid. The saving in storage requirements is one of the reasons that the first six-dimensional quantum dynamical treatment of hydrogen dissociation on surfaces was indeed a time-independent one using the LORE–INTRA scheme [50].

2.5. Classical dynamics

Once an analytical continuous representation of an ab initio PES is available, it is also possible to determine the gradients of the potential analytically. This allows one to perform ab initio molecular dynamics studies by integrating the classical equations of motion,

$$M_i \frac{\partial^2}{\partial t^2}\mathbf{R}_i = -\frac{\partial}{\partial \mathbf{R}_i} V(\{\mathbf{R}_j\}). \tag{21}$$

The solution of the equations of motion can be obtained by standard numerical integration schemes like Runge–Kutta, Burlisch–Stoer or predictor–corrector methods (see, e.g., [115]). Sticking corresponds to a process in which statistically distributed particles hit the surface. This means that the determination of classical sticking probabilities requires an average over typically thousands of trajectories. The initial conditions can be chosen either by some Monte-Carlo sampling or by an equidistant sampling.

Most ab initio total-energy programmes based on plane-wave expansions also evaluate the gradients of the potential via the Hellmann–Feynman theorem [54,55]. With these forces the classical equations of motion can directly be solved. This "traditional" ab initio molecular dynamics scheme with the

determination of the forces on the fly has the advantage that it does not require the fitting of the ab initio PES to any analytical or numerical representation. This is especially advantageous if surface degrees of freedom play an important role in the dissociation process. On the other hand, every step of the numerical integration of the equations of motion requires a new ab initio total-energy calculation which is still rather time-consuming. Hence the number of trajectories obtainable in such a "during the journey" ab initio molecular dynamics simulation is limited to numbers well below 100 [57–60]. Such a simulation only makes sense if one can extract meaningful information from a low number of events. For the simulation of adsorption events this is usually not the case, but for desorption, where the particles originate from a small portion of the phase space, "on the fly" ab initio molecular dynamics simulations can still be useful [58].

But even if an analytical representation of the ab initio PES is available, there is still some computational effort to determine dissociation probabilities. It is a wide-spread believe that classical dynamical methods are much less time-consuming than quantum ones. This is certainly true if one compares the computational cost of one trajectory to a quantum calculation. The quantum calculations, however, take advantage of the delocalized nature of the wave functions. A beam of particles approaching the surface is described by a plane wave in the gas-phase that includes all impact points. Also a non-rotating molecule is represented by a $j = 0$ rotational state, where j is the rotational quantum number and which contains all orientations with equal probability. Hence the averaging over initial conditions is done automatically in quantum mechanics. Consequently, quantum dynamical simulations do not necessarily have to be more time-consuming than classical calculations, in particular if one considers the fact that in wave-packet calculations the dissociation probability for a whole range of energies is calculated in one run or that in a time-independent coupled-channel method the sticking and scattering probabilites of all open channels are determined simultaneously.

The crucial difference between quantum and classical dynamics is that in the quantum dynamics the averaging is done coherently while it is done incoherently in the classical dynamics. For heavier molecules this is apparently not important, but for hydrogen dissociation this has important consequences, as will be shown below.

3. Hydrogen dissociation on metal surfaces

After introducing the theoretical concepts necessary to perform ab initio dynamics calculations, I will now discuss applications. I start with the hydrogen dissociation on metal surfaces.

While the dissociation of hydrogen at simple or noble metals is usually hindered by a substantial energy barrier, transition metal surfaces are rather reactive, i.e., already at low kinetic energies the dissociative adsorption probability is often larger than 10%. This reactivity has been attributed to the local density of states (LDOS) of the partly filled d-band at the Fermi level [119,120] or close to the Fermi level [121,122] of the transition metals. Recent investigations have shown that the reactivity cannot be solely understood in terms of the LDOS at the Fermi level, but rather by the hybridization between molecular and metal states which involves the whole d-band [45,123,124].

In noble metals the d-band is filled, which leads to the existence of a significant barrier towards dissociative adsorption of hydrogen. First I will discuss the ab initio dynamics calculations for such an activated system, namely H_2/Cu which has been the benchmark system for the study of dissociative adsorption. Then I will address the dissociation on transition metal surfaces. For these latter systems

ab initio dynamics calculations have proven their power by demonstrating the hitherto underestimated efficiency of one particular dynamical mechanism, the steering. This section ends with a discussion of the influence of preadsorbates on the energetics and dynamics of hydrogen dissociation on metal surfaces.

3.1. Dissociation on simple or noble metals

The model system for the study of dissociative adsorption over the last years has been H_2/Cu. Many detailed experimental [125–129] as well as theoretical [5,6,13–15,34,16,18,31,32] dynamical investigations about this system exist. The early dynamical calculations were mostly performed on model potentials. Sometimes the used potential energy surfaces were derived from a small cluster calculation where the Cu surface had been modelled by a Cu_2 dimer [120], or the PES was obtained from approximate methods like the effective medium theory [18,31,32].

Then in 1994 there appeared two papers back-to-back in Physical Review Letters [39,40] which represented the first detailed determination of a multi-dimensional PES as a function of all six hydrogen degrees of freedom by density-functional calculations. First of all these calculations showed that one has to go beyond the local density approximation (LDA) for the treatment of the exchange–correlation effects in density-functional theory calculations. LDA calculations yield an almost vanishing barrier to dissociation although the experiments show that the height of this barrier should be about 0.5 eV [125–129]. By including gradient corrections in the exchange–correlation functional (the so-called generalized gradient approximation (GGA) [85]) the general agreement with the experiment is greatly improved. Fig. 1 shows the GGA minimum barrier for H_2/Cu(111) in a so-called elbow plot. The PES is plotted as a function of the H_2 center-of-mass distance from the surface and the interatomic H–H distance. The molecular orientation and the center-of-mass coordinates parallel to the surface are kept

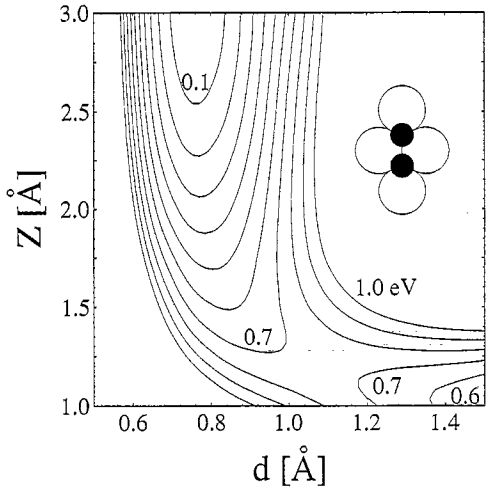

Fig. 1. Contour plot of the PES along a two-dimensional cut through the six-dimensional coordinate space of H_2/Cu(111) determined by DFT-GGA calculations. The inset illustrates the orientation of the molecular axis and the lateral H_2 center-of-mass coordinates, i.e. the coordinates X, Y, θ, and ϕ. The coordinates in the figure are the H_2 center-of-mass distance from the surface Z and the H–H interatomic distance d. Energies are in eV per H_2 molecule. The contour spacing is 0.1 eV. This cut corresponds to the minimum energy pathway (from [39]).

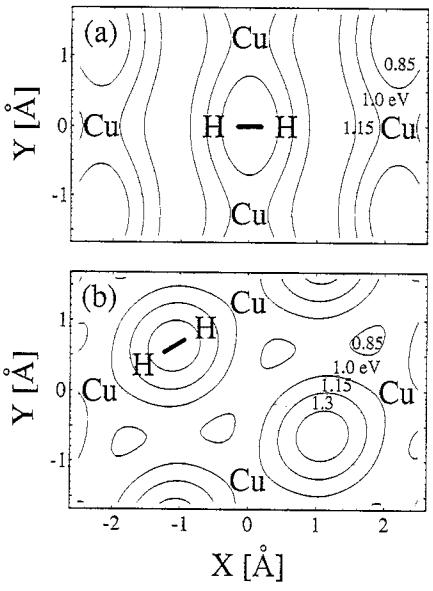

Fig. 2. The dissociation barrier height for H_2/Cu(111) as a function of the two lateral H_2 center-of-mass coordinates X and Y determined by DFT-GGA calculations. The positions of the copper substrate atoms are marked by "Cu". The molecular axis is parallel to the surface, its azimuthal orientation is illustrated by "H–H" (from [39]).

fixed. The calculations to determine the PES are not trivial; care has to be taken that the results are well-converged [39,130], and there are still some uncertainties about the exact barrier heights [40,130,131]. GGA represents a great improvement over LDA for certain systems as far as barrier heights are concerned, but it has its limitations [85,87], and the development of more accurate functionals is still going on (see, e.g., [86,132]).

The two papers [39,40] represented indeed a breakthrough in the determination of accurate and detailed potential energy surfaces. They challenged the gas–surface theorists with the fact that the interaction of hydrogen molecules with metal surfaces was much more corrugated than was anticipated before. Since the electronic density in front of metal surfaces is rather smeared out [119,133], it was assumed that the barrier for dissociation depends only very weakly on the location within the surface unit cell. This picture of a flat, structureless surface was seemingly confirmed by the experimentally found normal energy scaling of the sticking probability [125,129,134], i.e., the sticking probability is a function of the normal component of the incident kinetic energy alone.

The ab initio calculations, however, showed that the barrier to dissociative adsorption for the molecular axis parallel to the surface varies by 0.7 eV within the surface unit cell (see Fig. 2) [39]. The bond-breaking process even on metal surfaces is a very localized process close to the surface. It involves the hybridization of molecular orbitals with particular metal states, in particular d-states. These have a spatially strongly varying distribution reflecting their symmetry properties. For an illustration of the local character of this interaction see for example [122,135]. Hence it is the chemical nature of the dissociation process that leads to its spatial variation.

Motivated by the results of the ab initio calculations for the H_2/Cu PES, Darling and Holloway showed by using a three-dimensional model PES that strong corrugation can be reconciled with normal

energy scaling [22]. For this to happen, the higher barriers have to be further away from the surface than the lower ones. This "balanced" corrugation [38] was indeed found in the ab initio calculations [39,40].

Shortly after the publication of the ab initio H_2/Cu(111) PES the first high-dimensional dynamical calculations were performed [93] where the PES was entirely based on the first-principles calculations [39]. A five-dimensional parametrization of the ab initio PES has served as an input for the time-independent coupled-channel study. In this study the three center-of-mass coordinates and the interatomic spacing of the H_2 molecule have been treated quantum mechanically, while the azimuthal orientation of the molecule has been taken into account in a classical sudden approximation which works quite well in the H_2/Cu system [33].

These calculations demonstrated the importance of the multi-dimensionality for the determination of the sticking probability. Before, in the low-dimensional studies the barrier thickness has been used as a variable parameter in order to reproduce the slope of the sticking curve. In low-dimensional calculations the width of the increase is basically caused by tunneling for energies below the barrier height and by quantum back scattering for energies above the barrier height. Furthermore, mixed quantum–classical calculations of the sticking probability for H_2/Cu obtained by effective medium theory [31,32] showed only a modest dependence of the width of the sticking curve on the dimensionality of the calculations. The five-dimensional calculations on the GGA-PES demonstrated that only in the tunneling regime the rise of the sticking probability is determined by the barrier thickness [93]. Fig. 3 shows the results for the calculated sticking probabilities of these five-dimensional calculations. They are also compared to two-dimensional calculations that included only the minimum energy path geometry plotted in Fig. 1. For energies above the minimum barrier height the results of the two-dimensional and the five-dimensional calculations are very different. In this regime it is the whole barrier distribution that determines the width of the sticking curve. In the tunneling regime, on the other hand, the sticking curves of the two-dimensional and the five-dimensional calculations are just shifted (Fig. 3(b)) demonstrating that in this regime it is indeed the minimum barrier thickness that governs the adsorption dynamics.

As mentioned above, in the low-dimensional studies it was basically the barrier width that determined the rise of the sticking probability with kinetic energy. To reproduce the gradual increase of the experimental results, small barrier widths had to be assumed which were much smaller than the results obtained in the GGA calculations. In addition, to account for the experimental fact that vibrational excitation of the impinging molecules is very efficient for increasing the sticking probability [125], a late barrier after a strongly curved region according to Polanyi's rules [136] had been assumed in the model PES [5,6,10]. The curvature of the reaction path in the GGA-PES (Fig. 1) is much smaller than was previously assumed. It is not only the curvature, but also the lowering of the vibrational frequency in the barrier region, which on the other hand was underestimated before, that causes the vibrational effects in the dissociation process [137].

With regard to the effect of additional parallel momentum, Fig. 3 shows that for non-normal incidence the sticking probabilities fall upon the normal incidence sticking curve if they are plotted versus the normal kinetic energy for kinetic energies larger than 0.6 eV, i.e. in the regime where sticking is classically possible. The GGA-PES indeed shows the topological features necessary for normal energy scaling [22], namely the balanced corrugation [38] with the larger barriers further away form the surface than the smaller. The five-dimensional-calculations thus confirm the three-dimensional model calculations [22] with respect to the role of the surface corrugation.

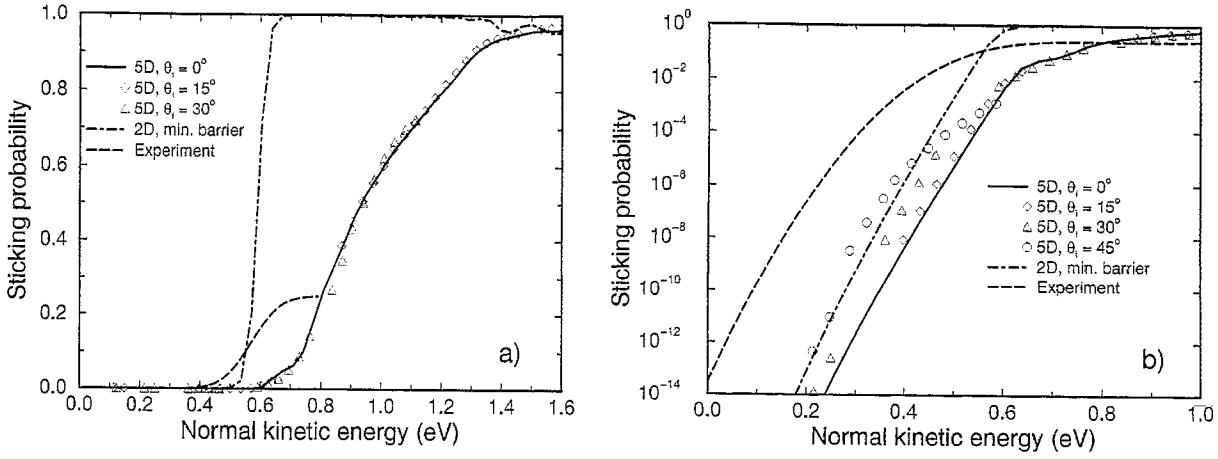

Fig. 3. Sticking probability versus normal kinetic energy of H_2/Cu(111) for molecules initially in the vibrational ground state: (a) linear plot; (b) logarithmic plot (note the different energy range). Five-dimensional-calculations for different incidence angles at the corrugated surface: solid line $\theta_i = 0°$, ◇ $\theta_i = 15°$, △ $\theta_i = 30°$, ◯ $\theta_i = 45°$; Dash–dotted line: two-dimensional-calculations corresponding to a flat surface with the minimum barrier (from [93]). Dashed line: Experimental curve (from [126]).

However, for the tunneling regime Fig. 3(b) reveals that additional parallel momentum enhances sticking. This is seemingly at variance with the molecular beam adsorption experiments in which normal energy scaling has been found for all energies in the system H_2/Cu(111) [125,126]. However, this apparent discrepancy can be explained by the fact that at low kinetic energies sticking in the beam experiments is dominated by the vibrationally excited molecules, and for these molecules the range where normal-energy scaling is obeyed is shifted to lower energies [111]. In very recent experiments [138] the state resolved angular dependence of the sticking probability of H_2/Cu(111) has been determined by applying detailed balance arguments to desorption experiments. Indeed, these experiments confirmed the theoretical prediction that additional parallel momentum enhances the sticking probability in the tunneling regime. In this tunneling regime the classical conception of particles moving like bob-sleds in a corrugated potential does not apply any more. The shortest propagation path through the barrier region is exponentially preferred with respect to all other paths. This shortest path usually corresponds to normal propagation through the barrier for a corrugated potential. Due to the corrugation parallel momentum can be efficiently transferred to normal momentum for tunneling particles, and this causes the enhancement of the sticking probability for additional parallel momentum in the low-energy regime.

The GGA-PES for H_2/Cu(111) of Hammer and coworkers served also as an input for three-dimensional wave-packet calculations [94] in which, besides the H_2 center-of-mass distance from the surface, one H_2 center-of-mass coordinate parallel to the surface and the polar orientation of the molecule were considered. The change of the vibrational frequency was taken into account by keeping the molecule adiabatically in its vibrational ground state. This study particularly focused on the difference between the results of quantum and classical calculations. Fig. 4 shows the dissociation probability as a function of the kinetic energy for energies close to the minimum barrier height. Classical and quantum results are shown for the two hydrogen isotopes H_2 and D_2. The difference between the two isotopes is due to the decrease in the zero-point vibrational energy during the

dissociation process. Since the vibrational frequency of D_2 is smaller by a factor of $1/\sqrt{2}$ than the H_2 frequency, for D_2 less vibrational energy is transferred to the translational degree of freedom leading to the smaller dissociation probability.

Rather surprising is the fact that for energies close to the dissociation barrier $E \approx 0.65$ eV the classical probabilities are larger than the quantum ones. Naively one would expect that the quantum results should be larger due to tunneling which is absent in the classical calculations. However, the PES is corrugated and anisotropic. For energies close to the minimum barrier energy only a limited range of molecular orientations and lateral coordinates are energetically accessible at the barrier position. The localization of the wave function in the angular and lateral degrees of freedom during the crossing of the minimum barrier region leads to the building up of zero-point energies in the quantum calculations. These zero-point energies cause an effective increase of the barrier height in the quantum dynamics which reduces the quantum dissociation probability compared to the classical probability. The zero-point energies also cause quantization effects in the dissociation probability at higher energies which are visible as a weak step-like structure in Fig. 4.

Just recently the first six-dimensional wave-packet studies of the dissociation of H_2 on Cu have appeared [52] which confirmed the importance of the multi-dimensionality for the dissociation process. Fig. 5 shows the results for the sticking probability of H_2 on Cu(1 0 0) [52]. The calculations were based on an analytical fit to the PES obtained by density functional theory using GGA. The wave-packet method used a symmetry-adapted basis set in the center-of-mass degrees of freedom parallel to the surface and for the molecular orientation. This causes a significant computational saving for initial conditions corresponding to normal incidence. Six-dimensional wave-packet calculations for non-normal incidence have not been performed yet. The theoretical results show some structure, in particular close to the threshold at 0.4 eV. These oscillations are attributed to resonances caused by the weakening of the molecular bond close to the surface [52].

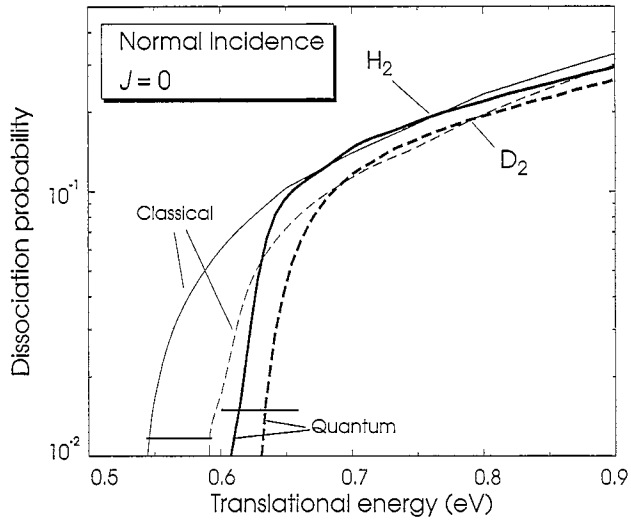

Fig. 4. Classical and quantum dissociation probability as a function of kinetic energy for initially non-rotating H_2 and D_2 molecules under normal incidence at Cu(111), determined by three-dimensional wave-packet calculations [94]. In these calculations the center-of-mass distance from the surface, one center-of-mass coordinate parallel to the surface and the polar orientation of the molecule were taken into account.

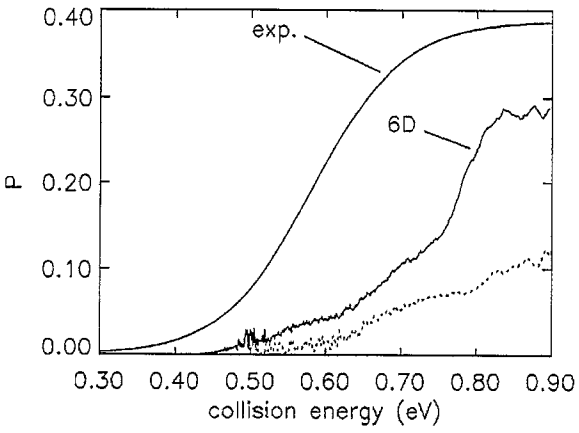

Fig. 5. Sticking probability for H_2 dissociation on Cu(1 0 0) determined by six-dimensional time-dependent quantum calculations on an ab initio PES (from [52]). The experimental data are taken from [134]. The dotted line shows the calculated probability for vibrational excitation in scattering.

The six-dimensional sticking curve seems to be shifted by roughly 0.2 eV to higher energies with respect to the experimental results. A similar shift is found in the five-dimensional calculations for H_2/Cu(111) in Fig. 3. This suggests that the GGA calculations overestimate the dissociation barriers. For H_2/Cu(111), convergence tests of the ab initio calculations suggested that the barriers should be lowered by 0.2 eV [39]; the inclusion of the polar orientation, which was not considered in the five-dimensional calculations, would shift the sticking curves to higher energies again, though.

On the other hand, the sticking probability is directly measured only for kinetic energies up to approximately 0.5 eV. H_2 beams with higher kinetic energies cannot be prepared in nozzle experiments. The experimental sticking probabilty for higher kinetic energies is derived from desorption experiments invoking the principle of detailed balance or microscopic reversibility. Because of this indirect procedure, for example the saturation value of the sticking probability, i.e. the maximum value at high energies, is not well-established experimentally; it has an uncertainty of a factor of two [126]. Hence it is not entirely clear yet, whether the discrepancy between theory and experiment is caused by experimental uncertainties or by approximations in the calculations.

Another six-dimensional time-dependent dynamical study is devoted to the dissociation of H_2 on Cu(111) [139]. However, this study is not fully based on an ab initio PES. The authors claim that the available ab initio information is not complete enough, however, they have not collaborated with any group that is able to perform ab initio total-energy calculations. They use an LEPS potential for the parametrization of the H_2 interaction with Cu(111). The LEPS parametrization is considered by other authors [47] to be not flexible enough to accurately describe the PES.

Although already many detailed studies exist about the system H_2/Cu, experimentally as well as theoretically, there is still room for further explorations in this system. For example, current experimental studies have focused on the rotational alignment of desorbing molecules [140–142]. These investigations address the issue of the anisotropy of the dissociation barriers. Another noble metal system under current interest is the dissociation of hydrogen on silver. Detailed experimental data exist for this system [143, 144], and just recently also the PES for H_2/Ag(1 0 0) was determined by first-principles calculations [135]. Hence there are still interesting results to be anticipated for the interaction of hydrogen with noble or simple metal surfaces.

3.2. Dissociation on transition metals

Molecular beam experiments of the dissociative adsorption of H_2 on Pd(1 0 0) have found that the sticking probability initially decreases with increasing kinetic energy of the beam [145,146]. Similar results have been obtained for the H_2 dissociation on various other transition metal surfaces [145,147–152]. Such a behavior is usually found for atomic or non-dissociative molecular adsorption in which the particles have to dissipate their excess energy to the substrate in order to remain on the surface [1]. Since the energy transfer to the substrate becomes less efficient at higher energies, the sticking probability for atomic or molecular adsorption decreases with increasing energy. Consequently a similar process has been invoked to explain a decreasing sticking coefficient in *dissociative* adsorption, namely the precursor mechanism: before dissociation the molecules are temporarily trapped in a molecular adsorption state, the so-called precursor state. This trapping probability which decreases with increasing energy is supposed to be the rate-determining step.

However, for hydrogen adsorption the large mass mismatch between adsorbate and substrate should make the energy transfer process inefficient. For the system H_2/W(1 0 0)–c(2×2)Cu, e.g., it was shown [151] that for a hydrogen molecule impinging on a metal substrate the energy transfer to substrate phonons is much too small to account for the high sticking probability at low kinetic energies.

Furthermore, density-functional theory calculations within the GGA found that there exist non-activated as well as activated paths to dissociative adsorption in the system H_2/Pd(1 0 0), but the calculations gave no indication of any molecular adsorption well, i.e. any precursor state [41,42]. Two elbow plots of the H_2/Pd(1 0 0) PES determined in these calculations are shown in Fig. 6. Fig. 6(a) demonstrates that the dissociative adsorption of H_2 on Pd(1 0 0) is non-activated, i.e. reaction pathways without any hindering barrier exist. For the conditions of Fig. 6(b), where the molecule approaches the surface at the on-top site, a barrier of approximately 0.15 eV exists. There seems to be a molecular adsorption well in front of the on-top site, but detailed calculations have shown that this well does not correspond to a local minimum of the PES [42]. It is rather a saddle point of the PES in the multi-dimensional configuration space because the molecule can still follow a purely attractive path to dissociative adsorption if its center-of-mass degrees of freedom are allowed to relax.

According to these theoretical results, the precursor mechanism cannot be operative in the H_2/Pd(1 0 0) system. As an alternative explanation it had been suggested that a decreasing sticking coefficient could be caused by a steering effect in a direct non-activated adsorption process by King twenty years ago [153], but there had been no theoretical confirmation whether this mechanism could be efficient enough. In classical stochastic molecular dynamics simulations it was demonstrated how the anisotropy and corrugation could lead to a focusing of the dissociating molecules to reactive sites, but the energy dependence of this process was not analyzed [28]. Furthermore, in two-dimensional dynamical treatments of the H_2/Pd(1 0 0) system no steering effect was observed [7,8,110].

The first dynamical evidence that the co-existence of non-activated with activated pathways to dissociative adsorption can lead to an initially decreasing sticking probability was found in three-dimensional quantum dynamical calculations [26]. In this study a model PES with features derived from the GGA calculations of H_2/Pd(1 0 0) [41] was used. However, still large quantitative discrepancies to the experiment remained, as far as the relevant energy range in which steering is operative was concerned.

Using a parametrization of the ab initio PES [41,42] based on 250 different configurations, six-dimensional dynamical calculations of the dissociative adsorption and associative desorption of

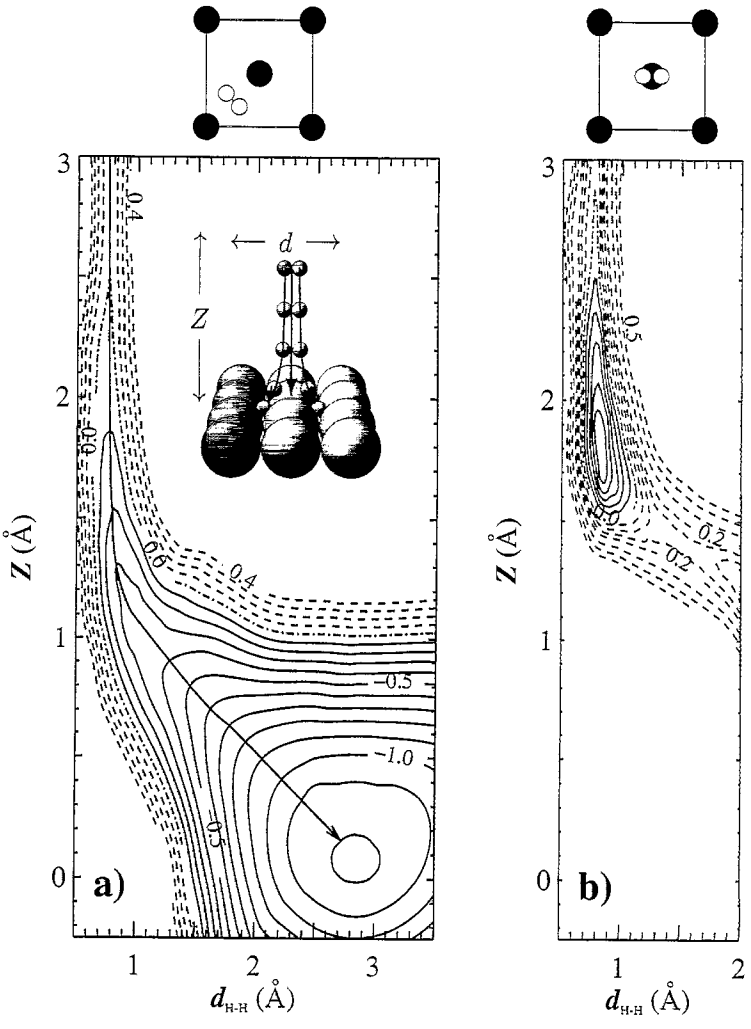

Fig. 6. Contour plots of the PES along two two-dimensional cuts through the six-dimensional coordinate space of H_2/Pd(1 0 0), so-called elbow plots, determined by GGA calculations [41,42]. The coordinates in the figure are the H_2 center-of-mass distance from the surface Z and the H–H interatomic distance d. The dissociation process in the Zd plane is illustrated in the inset. The lateral H_2 center-of-mass coordinates in the surface unit cell and the orientation of the molecular axis, i.e. the coordinates X, Y, θ, and ϕ are kept fixed for each two-dimensional cut and depicted above the elbow plots. Energies are in eV per H_2 molecule. The contour spacing in (a) is 0.1 eV, while it is 0.05 eV in (b).

H_2/Pd(1 0 0) have been performed [50]. These calculations were indeed the first in which all six degrees of freedom of the hydrogen molecule were treated quantum dynamically. Fig. 7 presents the six-dimensional results of the sticking probability of H_2/Pd(1 0 0) under normal incidence. These results are compared to the H_2 molecular beam adsorption experiment by Rendulic et al. [145]. Furthermore, the experimental results of Rettner and Auerbach [146] for a reflection beam experiment under an angle of incidence of $\theta_i = 15°$ are plotted.

First of all, a strong oscillatory structure is evident in the quantum results. Such oscillations have also been found in four-dimensional wave-packet calculations of H_2/W(1 0 0) [61] which is also a reactive

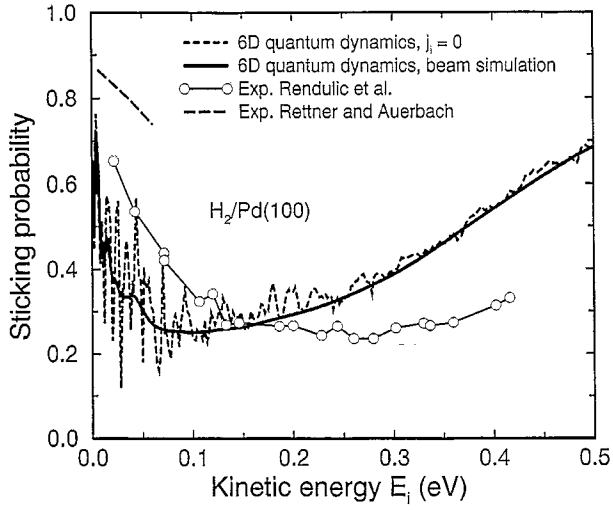

Fig. 7. Sticking probability versus kinetic energy for a hydrogen beam under normal incidence on a Pd(1 0 0) surface. Theory: six-dimensional quantum calculations for H_2 molecules initially in the rotational and vibrational ground state (dashed line) and with an initial rotational and energy distribution adequate for molecular beam experiments (solid line) [50]. H_2 molecular beam adsorption experiment under normal incidence (Rendulic et al. [145]): circles; H_2 effusive beam scattering experiment with an incidence angle of $\theta_i = 15°$ (Rettner and Auerbach [146]): long-dashed line.

system; those were, however, smaller. It has been shown that the energetic location of most of the peaks, in particular at low kinetic energies, can be related to the opening of new scattering channels with increasing kinetic energies, i.e. they correspond to threshold effects [154,155]. In the case of the diffraction channels, the energetic position of the peaks is thus fully determined by the geometry of the surface. Their size depends sensitively on the symmetry of the initial conditions. For normal incidence they are much more pronounced than for non-normal incidence because the number of degenerate, symmetrically equivalent scattering channels is reduced for non-normal incidence [51,155]. Holloway and coworkers have recently shown [156] that the size of the oscillations also depends on the specific topology of the PES, in particular on the existence of possible resonance states in front of the surface.

Rettner and Auerbach have searched for these oscillations in a reflection experiment using a nearly effusive beam [146,157]. This kind of experiment allows a high energy resolution of the total scattering probability [158]. They have not found any indication of these oscillations. However, this is not an easy experimental task since surface impurities and the increasing hydrogen coverage during the scattering experiment destroy the coherence of the scattering event and suppress the oscillations. Furthermore, they have used an angle of incidence of 15° instead of normal incidence which also causes a suppression of the oscillations [51], since the symmetry of the initial conditions has a decisive influence on the magnitude of the oscillations. Simulated time-of-flight (TOF) distributions for H_2 scattered at Pd(1 0 0) with the same angle of incidence as used in the experiment are very close to the experimental TOF distributions [51]. The results of Rendulic et al. [145] do not show any strong oscillatory structure either, but for an additional reason. An experimental molecular beam does not correspond to a monoenergetic beam in one specific quantum state. If one assumes an energy spread and a distribution of internal molecular states typical for a beam experiment, the oscillations are almost entirely smoothed out in the six-dimensional quantum results (solid line in Fig. 7).

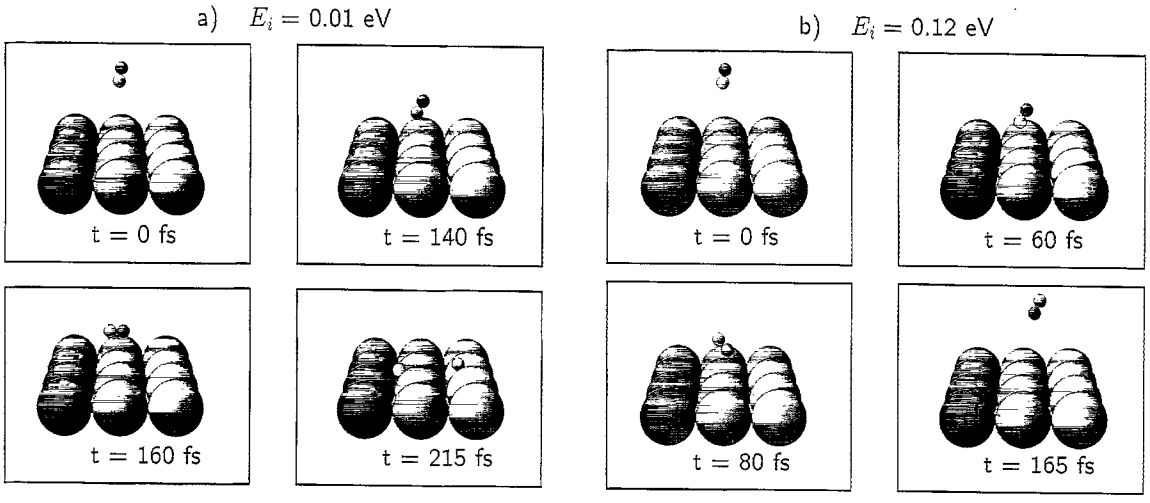

Fig. 8. Snapshots of ab initio molecular dynamics trajectories for H_2 molecules impinging on Pd(1 0 0) in order to illustrate the steering effect. The molecules are initially not vibrating and not rotating. For both trajectories the initial conditions are the same, except for the kinetic energy which is 0.01 eV in (a) and 0.12 eV in (b).

The general agreement between theory and the experiments is satisfactory. As noted above, the ab initio PES does not have any molecular adsorption well, i.e., no precursor state. In addition, due to the fact that the substrate is kept fixed, no energy transfer to the surface is taken into account in the calculations. Still the initial decrease of the sticking probability found in the experiments is well-reproduced in the quantum dynamical calculations. Such an initial decrease of the sticking probability has also been found in classical molecular dynamics calculations on the same PES [51,159] and in quantum and classical calculations of the sticking probability of H_2/W(1 0 0), too [61]. Hence the underlying microscopic mechanism that is responsible for the decrease can also be investigated by analyzing classical trajectories. This analysis yields that the large sticking probability at low kinetic energies is caused by the steering effect that becomes less efficient at higher kinetic energies which then leads to the decrease of the dissociation probability.

Fig. 8 illustrates this general mechanism by showing snapshots of two ab initio molecular dynamics runs. For both trajectories initially non-vibrating and non-rotating molecules impinge on the surface under the same conditions except for the initial kinetic energy which is 0.01 eV in Fig. 8(a) and 0.12 eV in Fig. 8(b). Far away from the surface the molecular axis is oriented almost perpendicular to the surface. In such an orientation the molecule cannot dissociate, the interaction with the surface is repulsive. The PES is, however, strongly anisotropic, and there are forces acting on the molecule to orient it to a parallel configuration to the surface. If the molecule is slow enough, as in Fig. 8(a), it can indeed complete the rotation into this favorable orientation before hitting the repulsive wall of the potential. Close to the surface, after 160fs, the molecule has turned parallel to the surface and directly dissociates from this configuration. This process becomes less efficient at higher kinetic energies which is demonstrated in Fig. 8(b) where the initial kinetic energy is 12 times larger. Of course the same forces act upon the molecule, but now the molecule is too fast to be fully re-oriented. It hits the surface in an unfavorable configuration in which the interaction is repulsive. At the classical turning point there is a very rapid rotation corresponding to a flip–flop motion, and then the molecule is scattered back into

the gas-phase rotationally excited. By further increasing the kinetic energy, the molecules will eventually have enough energy to directly traverse the barrier region which causes the final increase in the sticking probability (see Fig. 7).

The events that are depicted in Fig. 8, direct dissociation or direct reflection, only correspond to the two limits of the possible outcome of a scattering event. A slow molecule approaching the surface can start rotating caused by the anisotropy of the PES without directly dissociating. Due to the conversion of translational energy into rotational energy it might lose so much translational energy that it cannot escape into the gas phase again. The corrugation of the surface can also cause motion parallel to the surface. In such a state the molecule is trapped into a dynamical precursor, which is *not* caused by energy transfer to the substrate but by energy transfer to rotational and kinetic energy of the molecule parallel to the surface. In ab initio molecular dynamics calculations adsorption events have been found in which the molecule spent more than 5 ps in front of the surface before dissociating [159]. Note that such events correspond to the existence of metastable states in quantum scattering. These are very sensitive to the specific topology of the PES [156].

Both the trapping into a molecular adsorption state by energy dissipation to the substrate and the suppression of the steering effect lead to a sticking probability that decreases with increasing kinetic energy. It is therefore desirable to find experimental properties that allow an unambiguous distinction between these two different mechanisms. As such a property the dependence of the sticking probability on the initial rotational motion of the molecules has been suggested [160]. One of the properties of the PES that leads to steering, the anisotropy of the potential, also causes a suppression of the sticking probability when the molecules are rapidly rotating. Molecules with a high angular momentum will rotate out of a favorable orientation towards dissociative adsorption during the time it takes to break the molecular bond. This is shown in Fig. 9 where the six-dimensional sticking probability for a kinetic energy of $E_i = 10$ meV as a function of the initial rotational state is plotted. The diamonds correspond

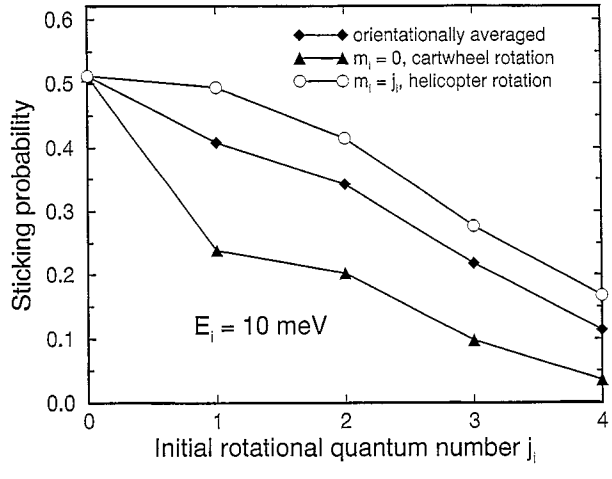

Fig. 9. Sticking probability versus initial rotational quantum state j_i for the system H_2/Pd(1 0 0). Diamonds: orientationally averaged sticking probability (Eq. 22), triangles: $m_i = 0$ (cartwheel rotation), circles: $m_i = j_i$ (helicopter rotation). The initial kinetic energy is $E_i = 10$ meV.

to the orientationally averaged sticking probability

$$\bar{S}_{j_i}(E) = \frac{1}{2j_i+1} \sum_{m_i=-j_i}^{j_i} S_{j_i,m_i}(E). \tag{22}$$

The strong decrease with increasing initial rotational quantum number j_i is caused by a suppression of the steering effect. Fast rotating molecules cannot be focused into a favorable orientation towards adsorption, they will be reflected from the surface.

It is not easy to prepare experimentally a molecular beam in a single quantum state. Still, this rotational hindering of the steering effect has actually been confirmed for H_2/Pd(111) [161,162] and also for H_2/Pt(110) [163]. By seeding techniques the translational energy of a H_2 beam can be changed in a nozzle experiment without altering the rotational population of the beam [161,162]. Also the different sticking probabilities of para- and *n*-hydrogen beams have been used to extract information about rotationally resolved results [163]. Fig. 10 shows the results of a seeded beam experiment for H_2/Pd(111) by Beutl and coworkers [161]. The seeded beams have larger rotational energies than the unseeded beam at the same kinetic energies. It is said, they are rotationally hot. Indeed, especially at low kinetic energies the predicted strong suppression of the sticking probability by the rotational hindering is found, see Fig. 10.

According to the principle of detailed balance, the suppresion of the sticking probability by the rotational hindering should be reflected by a population of rotational excited states in desorption which is lower than expected for molecules in thermal equilibrium with the surface temperature. This so-called rotational cooling has indeed been found for H_2 molecules desorbing from Pd(1 0 0) [164,165] and is also well reproduced by the six-dimensional quantum dynamical calculations [50].

In the precursor mechanism the molecules are assumed to be first trapped in a physisorption state. Such a state is caused by van-der-Waals forces which depend only weakly on the orientation of the molecule. Hence there are only small directional forces, and molecules adsorbed in such a physisorption state are able to rotate almost freely [1,166]. The trapping probability into the

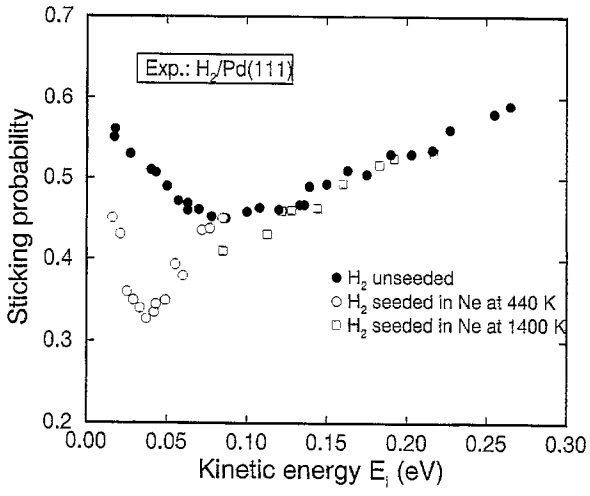

Fig. 10. Experimental sticking probability versus kinetic energy for a H_2 beam under normal incidence on a Pd(111) surface. The seeded beams have larger rotational energies at identical kinetic energies than the unseeded beam (after [161]).

physisorption state and thus the sticking probability in the precursor model should therefore be almost independent of the initial rotational state, in contrast to the steering mechanism. In another series of experiments Beutl and coworkers have measured the dependence of the sticking probabilities on the initial rotational energies in the "classical" precursor systems N_2/W(1 0 0), CO/FeSi(1 0 0) and O_2/Ni(111) [167]. They found no discernible influence of the rotational motion on the sticking coefficient in these systems. Hence the rotational dependence might indeed serve as a means to distinguish between the precursor mechanism and the steering effect.

So far all the results presented were averaged over the azimuthal quantum number m, i.e, the results corresponded to orientationally averaged properties. Now the H_2/Pd(1 0 0) PES is strongly anisotropic with regard to the molecular orientation. The most favorable configuration towards dissociative adsorption is with the molecular axis parallel to the surface. Molecules that hit the surface in an upright position cannot dissociate, they are reflected back into the gas-phase. It is true that quantum mechanics does not allow for non-rotating, oriented molecules in the gas-phase, however, rotating molecules can show a preferential orientation. Fig. 9 also shows the effect of molecular orientation on the sticking probability. Molecules with azimuthal quantum number $m = j$ have their axis preferentially oriented parallel to the surface. These molecules rotating in the so-called helicopter fashion dissociate more easily than molecules rotating in the cartwheel fashion ($m = 0$) with their rotational axis preferentially parallel to the surface since the latter have a high probability hitting the surface in an upright orientation in which they cannot dissociate.

Experimentally it is hard to align a molecular beam of hydrogen. Again one can study the time-reverse process, the associative desorption. By laser-induced fluorescence (LIF) it is possible to measure the rotational alignment parameter $A_0^{(2)}(j)$ [168], which is given by

$$A_0^{(2)}(j) = \left\langle \frac{3J_z^2 - \mathbf{J}^2}{\mathbf{J}^2} \right\rangle_j . \tag{23}$$

$A_0^{(2)}(j)$ corresponds to the quadrupole moment of the orientational distribution and assumes values of $-1 \leq A_0^{(2)}(j) \leq 2$. Molecules rotating preferentially in the cartwheel fashion have an alignment parameter $A_0^{(2)}(j) < 0$, for molecules rotating preferentially in the helicopter fashion $A_0^{(2)}(j) > 0$.

Experiments have in fact found a preferential population of the helicopter mode in the desorption of D_2/Pd(1 0 0) [169]. Fig. 11 shows a comparison of these experimental results for D_2 with the six-dimensional calculation of the rotational alignment of H_2 desorbing from a Pd(1 0 0) surface at a surface temperature of $T_s = 690$ K [170]. Experimentally there is no big difference in the alignment factors as a function of the rotational quantum number j between H_2 and D_2 [171], hence the comparison is meaningful. The agreement for $j \leq 6$ is quite satisfactory. Indeed the molecules desorb preferentially with their molecular axis parallel to the surface thus reflecting the anisotropy of the PES. Due to computational restrictions the rotational alignment could only be calculated for $j \leq 6$. For $j = 7$ and $j = 8$ the experiments show a vanishing alignment within the error bars which is rather surprising. It was argued that for these high rotational states an energy transfer from the rotations to the reaction coordinate could suppress the effect of the potential anisotropy [169]. Certainly these results deserve further clarification.

The dependence of adsorption and desorption on kinetic energy, molecular rotation and orientation [50,160], molecular vibration [137], ro-vibrational coupling [170], angle of incidence [51], and the rotationally elastic and inelastic diffraction of H_2/Pd(1 0 0) [155] have been studied so far by six-

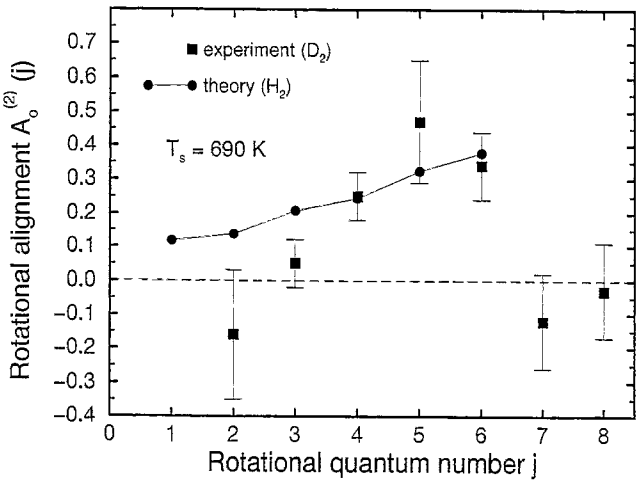

Fig. 11. Rotationally alignment of hydrogen molecules desorbing from a Pd(1 0 0) surface. Boxes: experimental results for D_2 [169]. Circles: six-dimensional quantum dynamical calculations for H_2 (from [170]).

dimensional ab initio dynamics calculations on the same PES. The results of these calculations have been compared to a number of independent experiments, and they are at least in semi-quantitative agreement with all of these experiments. Recently six-dimensional ab initio quantum dynamical calculations of H_2/Pd(1 0 0) have been performed [66,172] which were based on a much larger set of DFT-GGA calculations [135]. This allowed a more detailed analytical representation of the PES and significantly improved the agreement between theoretical and experimental sticking probabilitities [66,172]. This shows that ab initio dynamics calculations are capable of adequately describing the hydrogen dissociation on transition metal surfaces. In addition, the difference between six-dimensional ab initio quantum dynamics and classical dynamics has been addressed [159]. As in the case of the three-dimensional-calculations of the hydrogen dissociation on Cu(111) (see Fig. 4) the crucial difference between classical and quantum dynamics is not due to tunneling, but to zero-point effects. However, caused by the higher dimensionality of the six-dimensional-calculations the number of zero-point vibrational modes perpendicular to the reaction path is larger which makes the difference between classical and quantum results much more pronounced. This shows that a proper inclusion of zero-point effects is required in the treatment of hydrogen dynamics. I will address this issue in more detail in Section 3.3 about the hydrogen dissociation on an adsorbate covered surface.

It is also well-known that palladium is able to absorb large amounts of hydrogen in the bulk and can therefore be used for hydrogen storage [173]. The process of how hydrogen might enter the bulk has been the issue of ab initio quantum dynamics studies employing two- and three-dimensional wave-packet calculations by Olsen et al. [174,175]. In order to determine the effect of surface motion on direct subsurface absorption of H_2/Pd(111) they have calculated a GGA-PES depending on two hydrogen and one palladium degree of freedom [175]. They found that indeed the surface degrees of freedom play an important role at low kinetic energies as surface relaxation can lower the effective barrier towards direct subsurface absorption substantially. Still this barrier is too large to explain the experimentally observed direct subsurface absorption [176], probably due to the restricted dimensionality of these calculations, so that higher-dimensional calculations are desirable.

3.3. Dissociation on an adsorbate covered metal surface

The presence of an adsorbate on a surface can profoundly change the surface reactivity. An understanding of the underlying mechanisms and their consequences on the reaction rates is of decisive importance for, e.g., designing better catalysts. Traditionally a "trial and error" approach was used to improve the activity of a catalyst by adding some substances. Only recently this problem has been addressed theoretically by ab initio methods [177].

On Pd(1 0 0) it is experimentally well-known that the presence of sulfur leads to a large reduction of the hydrogen dissociation probability [145,178], it "poisons" the dissociation. While at the clean surface the dissociation probability is about 60% for a kinetic energy of $E_i = 0.05$ eV, at the sulfur-covered surface it drops below 1% at the same energy [145].

DFT-GGA calculations have shown that hydrogen dissociation on sulfur-covered Pd(1 0 0) is still exothermic, however, the dissociation is hindered by the formation of energy barriers in the entrance channel of the potential energy surface (PES) [43]. Fig. 12 shows two elbow plots of an analytical fit to the GGA-PES of H_2 at the (2×2) sulfur covered Pd(1 0 0) surface for fixed molecular orientation and lateral center-of-mass coordinates of the molecule. The minimum energy path is shown in Fig. 12(a). The molecule approaches the surface above the fourfold hollow site. This is the site where the H_2 molecule is furthest away from the sulfur atoms on the surface. An analysis of the electronic structure calculations has revealed that the building up of the barrier at this position is not related to a direct interaction between sulfur and the hydrogen molecule. Instead, it is caused by the sulfur-mediated

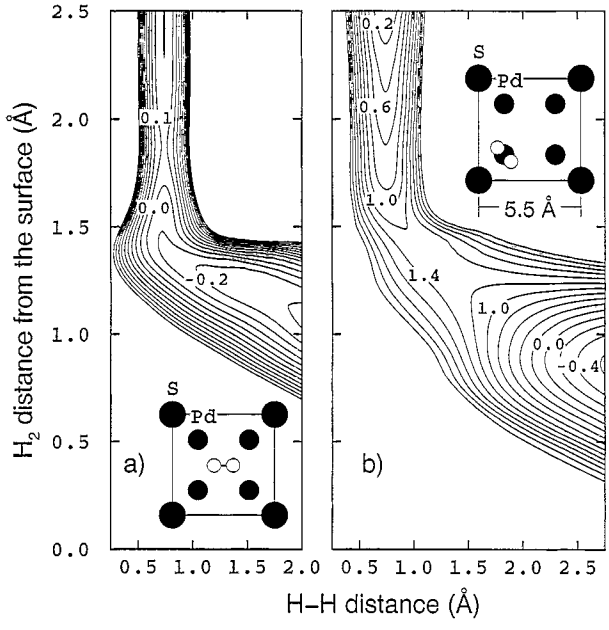

Fig. 12. Contour plots of the PES along two two-dimensional cuts through the six-dimensional coordinate space of H_2/S(2×2)/Pd(1 0 0). The insets show the orientation of the molecular axis and the lateral H_2 center-of-mass coordinates, i.e. the coordinates X, Y, θ, and ϕ. The coordinates in the figure are the H_2 center-of-mass distance from the surface Z and the H–H interatomic distance r. Energies are in eV per H_2 molecule. The contour spacing in (a) is 0.1 eV, while in (b) it is 0.2 eV. (a) corresponds to the minimum energy pathway.

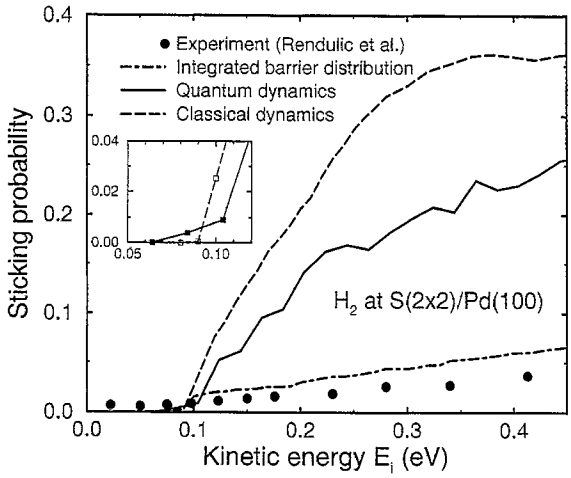

Fig. 13. Sticking probability versus kinetic energy for a H_2 beam under normal incidence on a S(2×2)/Pd(1 0 0) surface. Full dots: experiment (from [145]); dashed–dotted line: integrated barrier distribution, which corresponds to the sticking probability in the hole model [17]; solid line: quantum mechanical results for molecules initially in the rotational and vibrational ground-state; dashed line: classical results for initially non-rotating and non-vibrating molecules. The inset shows the quantum and classical results at low energies.

downshift of the Pd d-bands at the surface [43,44] which leads to a population of anti-bonding molecule-surface states [45].

Closer to the sulfur atoms the PES becomes strongly repulsive. This is illustrated in Fig. 12(b). While the dissociation path over the Pd on-top position on the clean surface is hindered by a barrier of height 0.15 eV [42], the adsorbed sulfur leads to an increase in this barrier height to 1.3 eV. Directly above the sulfur atoms the barrier towards dissociation even increases to values larger than 2.5 eV [44] for molecules oriented parallel to the surface. Here direct interaction between the sulfur atom and the H_2 molecule is responsible for the repulsion and the high barrier [44].

On the analytical representation of the PES of H_2 at the (2×2) sulfur covered surface six-dimensional dynamical calculations have recently been performed [103]. To my knowledge, this represents the most corrugated system of dissociative adsorption studied dynamically so far. Fig. 13 compares the quantum and classical results for the sticking probability as a function of the kinetic energy of the incident H_2 beam with the experiment [145]. In addition, also the integrated barrier distribution $P_b(E)$,

$$P_b(E) = \frac{1}{2\pi A} \int \Theta(E - E_b(\theta, \phi, X, Y)) \cos\theta \, d\theta \, d\phi \, dX \, dY \tag{24}$$

is plotted. Here θ and ϕ are the polar and azimuthal orientation of the molecule, X and Y are the lateral coordinates of the hydrogen center-of-mass. A is the area of the surface unit cell. Each quadruple defines a cut through the six-dimensional space (see Fig. 12 for examples), and E_b is the minimum energy barrier along such a cut. The function Θ is the Heavyside step function. The quantity $P_b(E)$ is the fraction of the configuration space for which the barrier towards dissociation is less than E; it corresponds to the sticking probability in the classical sudden approximation or the so-called "hole model" [17].

Table 1
Zero-point energies (ZPE) of the H_2 molecule at the minimum barrier position (the H_2 configuration corresponds to the situation of Fig. 12(a); the gas-phase zero-point energy of H_2 is $\frac{1}{2}\hbar\omega_{gas} = 0.258$ eV)

Mode	ZPE (eV)
H–H vibration	0.253
Polar rotation	0.016
Azimuthal rotation	0.013
Translation perpendicular to molecular axis	0.027
Translation parallel to molecular axis	0.027
Sum	0.336

The calculated sticking probabilities are significantly larger than the experimental results. The onset of dissociative adsorption at $E_i \approx 0.12$ eV, however, is well reproduced by the calculations. This onset is indeed also in agreement with the experimentally measured mean kinetic energy of hydrogen molecules desorbing from sulfur covered Pd(1 0 0) [179]. The theoretical results are relatively insensitive to variations in the barrier heights of the order of 0.2 eV [103]. It might therefore well be that uncertainties in the experimental determination are responsible for the difference. The exact sulfur coverage in the experiment was not very well characterized. The sulfur adlayer was obtained by simply heating up the sample which leads to segregation of bulk sulfur at the surface. The sulfur coverage was monitored through the ratio of the Auger peaks S_{132}/Pd_{330} [145]. The set of experimental data shown in Fig. 13 were obtained for half of the maximum segregation coverage of sulfur on Pd(1 0 0). This saturation coverage is assumed to be roughly $\Theta_S \approx 0.5$. Apart from uncertainties in this determination of the sulfur coverage also subsurface sulfur might have influenced the measurements. In [178] a linear decrease of the hydrogen saturation coverage with increasing sulfur coverages was found. At a sulfur coverage of $\Theta_S = 0.28$ hydrogen adsorption should be completely suppressed. This infers a site-blocking effect which is at variance with the ab initio calculations of the PES for this system [43,44]. However, these seemingly contradicting results and also the discrepancy between calculated and measured sticking probabilities could be reconciled if subsurface sulfur (which is not considered in the calculations but which might well be present in the experimental sample) has a decisive influence on the hydrogen adsorption energies. It is certainly desirable that the effect of subsurface sulfur on the hydrogen adsorption in this system will be investigated.

Fig. 13 shows furthermore that the classical molecular dynamics calculations over-estimate the sticking probability of H_2 at S(2×2)/Pd(1 0 0) compared to the quantum results. There are two important quantum phenomena not taken into account by classical calculations: tunneling and zero-point effects. For energies smaller than the minimum barrier height E_b the classical sticking probability is of course zero, whereas the quantum results still show some dissociation due to tunneling, as the inset of Fig. 13 reveals. But for energies larger than E_b the classical sticking probability rises to values which are almost 50% larger than the quantum sticking probabilities. Tunneling increases the quantum transmission probability with respect to the classical result, hence tunneling would have the opposite effect as observed in Fig. 13. Thus only zero-point effects can be responsible for the large difference [51,159].

Since the hydrogen molecular bond is still almost intact at the minimum barrier position, the H–H vibrational frequency should not be too different from its gas-phase value there. However, the minimum barrier is localized in the lateral coordinates parallel to the surface and in the rotational degrees of freedom of the molecule. The associated modes become "frustrated" which leads to zero-point energies in these degrees of freedom. This is confirmed by Table 1 where the zero-point energies of the hydrogen molecule at the minimum barrier position are collected. Note that the zero-point energies in the frustrated rotational and lateral modes are still small, in particular the rotational modes. This is caused by the fact that the molecular bond is essentially not elongated at the minimum barrier position so that the molecular interaction with the surface is still rather isotropic.

However, the sum of all zero-point energies at the minimum barrier position is in fact 0.08 eV larger than the gas-phase zero-point energy of hydrogen which is just half the molecular vibrational frequency $\frac{1}{2}\hbar\omega_{\mathrm{gas}} = 0.258$ eV. The combined effect of all zero-point energies at the minimum barrier position is to enlarge the effective barrier height by 0.08 eV to $E_{\mathrm{b}}^{\mathrm{eff}} = 0.17$ eV. The absence of zero-point effects in the classical dynamics causes the strongly enhanced sticking probability in the classical calculations. Still there is already a significant quantum sticking probability for kinetic energies below this effective barrier height. A detailed dynamical analysis suggests that this is due to the combined effect of steering and tunneling [180]. Classically steering does not help to traverse the barrier region for energies below the barrier height. Also for energies only slightly larger than the barrier height steering is not very efficient. This is different in quantum dynamics where steering can already occur in the tunneling regime. Therefore it is very effective for energies close to the minimum barrier height with respect to the classical results.

Although the dissociation of hydrogen on the sulfur covered Pd(1 0 0) surface in contrast to the clean surface is hindered by barriers, there is also significant steering of the impinging molecules to low-barrier configurations operative. This is reflected by the fact that the calculated sticking probabilities are much larger than what one would expect from the hole model [17] (see Fig. 13). This steering has been confirmed by analyzing swarms of trajectories and is illustrated in Fig. 14. The center-of-mass trajectories of H_2 molecules impinging on the diagonal of the unit cell of the (2×2) sulfur covered

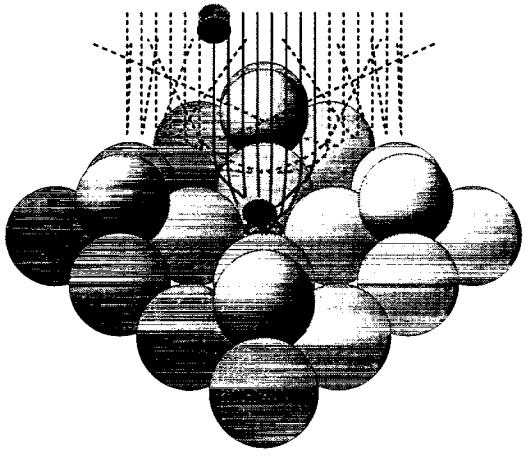

Fig. 14. Illustration of steering at the (2×2) sulfur covered Pd(1 0 0) surface. Center-of-mass trajectories of H_2 molecules are shown impinging with a kinetic energy of $E_{\mathrm{i}} = 0.3$ eV on the diagonal of the (2×2) unit cell. Dashed lines correspond to reflection events while the full lines depict adsorption events.

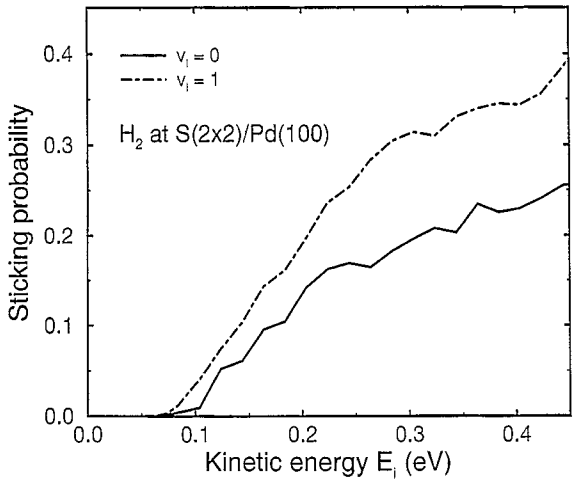

Fig. 15. Dependence of the quantum sticking probability versus kinetic energy for a hydrogen beam under normal incidence at a S(2×2)/Pd(1 0 0) surface on the initial vibrational state v. Solid line: $v_i = 0$, dash–dotted line: $v_i = 1$. The molecules are initially in the rotational ground state.

Pd(1 0 0) surface are shown. The initial kinetic energy is 0.3 eV. The molecular axis is parallel to the surface, but the initial azimuthal orientation is chosen in such a way that in the sudden approximation all initial conditions do not lead to dissociative adsorption since all incoming molecules hit barriers larger than 0.3 eV. The strongly repulsive potential directly above the sulfur atoms extends rather far into the gas-phase [44]. Incoming molecules are thus diverted from this high-barrier sites. Near to the sulfur atoms, the molecules are still scattered back into the gas-phase, but closer to the center of the (2×2) unit cell, the molecules are focused to the minimum barrier site. This focussing is accompanied by a reorientation of the molecular axis so that the molecule dissociates in the configuration depicted by the inset of Fig. 12(a).

The effect of initial vibrational motion on the dissociation process is demonstrated in Fig. 15 where state-specific sticking probabilities as a function of the incident kinetic energy are plotted. As Fig. 12(a) shows, the minimum barrier to dissociation is at a position where the bond-length of the molecule is still not significantly elongated. In such a situation it is usually anticipated that the vibrational and translational degrees of freedom are almost uncoupled so that vibrational energy of the impinging molecules cannot be used to overcome the barrier (see, e.g., [38]). Consequently, it has been predicted [43] that the sticking probability of H_2 at S(2×2)/Pd(1 0 0) should show no strong dependence on the initial vibrational state of the molecule. This prediction corresponds to the so-called Polanyi rules which have been formulated for gas-phase dynamics 30 years ago [136]. Apparently the rules have to be modified for strongly corrugated surfaces. Figure 15 demonstrates that initial vibrational excitation leads to a significant increase in the sticking probability in this early barrier system. As Fig. 12(b) reveals, there are molecular configurations for which the bond is significantly extended at the barrier position. Adsorbing molecules do not only probe the minimum barrier of the PES, but also other regions of the PES where vibrational energy can be efficiently used to overcome the dissociation barriers. This result of the vibrationally enhanced dissociation is actually in agreement with the experimentally observed vibrational over-population in thermal hydrogen desorption from sulfur covered Pd(1 0 0) [181] invoking the principle of microscopic reversibility.

It is interesting to note that the quantum sticking probability for molecules in the first excited vibrational state is close to the classical sticking probability for non-vibrating molecules (see. Fig. 13). For the hydrogen dissociation on the clean Pd(1 0 0) surface it has been shown that zero-point effects can cancel out of the dynamics calculations if the sum of all zero-point energies remains constant along the dissociation path [159]. For H_2 at S(2×2)/Pd(1 0 0) this sum increases as Table 1 shows. Now the H–H vibration corresponds to the fastest mode in the dissociation dynamics, and a comparison of five-dimensional vibrationally adiabatic with full six-dimensional calculations has shown that the vibrations indeed follow the change of the vibrational frequency during the dissociation almost adiabatically [137]. For molecules in the first excited vibrational state the transfer from vibrational energy to translational energy due to the lowering of the vibrational frequences can compensate the increase in the zero-point energies in the rotational and lateral modes leading to the described cancellation effect.

4. Hydrogen interaction with semiconductor surfaces

The ab initio studies of hydrogen dissociation on metal surfaces provide a rather complete picture of the dissociation process. The quantitative agreement can still be improved by, e.g., the inclusion of dissipation processes to substrate phonons or electron–hole pairs, the general mechanisms, however, seem to be understood (of course one should always be careful with such optimistic statements). For the interaction of hydrogen with semiconductor surfaces, on the contrary, there is still no general agreement on the fundamental mechanism, especially in the well studied system H_2/Si. The reason lies in the fact that the rearrangement of the semiconductor surface upon hydrogen adsorption can no longer be neglected as for metal systems. This makes the adsorption/desorption dynamics and their theoretical description more complicated.

In the following I will first discuss the dissociation dynamics of hydrogen on Si(1 0 0). Then I will address a recent ab initio study of the reaction of atomic hydrogen with the hydrogen-passivated Si(1 0 0) surface.

4.1. Dissociation on semiconductor surfaces

The system H_2/Si plays the same role for the hydrogen dissociation on semiconductors that H_2/Cu has for metal surfaces: it serves as a model system for which an abundance of experimental and theoretical studies exist (see for example the recent review by Kolasinski [56]). Besides, this system is also of great technological relevance for, e.g., the etching and passivation of Si surfaces or the growth of Si crystals.

Desorption of hydrogen from Si(1 0 0) shows first-order kinetics [182–185]. For associative desorption one normally expects second-order kinetics since two atoms have to find each other on the surface before they can desorb. The unusual first-order desorption kinetics has been explained by a prepairing mechanism [91,183,184]: Desorbing molecules originate from the same dimer since it is energetically favorable for two hydrogen atoms to bind on the same dimer rather than on two independent dimers (see Fig. 16(a)).

The so-called barrier puzzle has further fueled the interest for this system: While the sticking coefficient of molecular hydrogen on Si surfaces is very small [186–189] indicating a high barrier to adsorption, in a laser-induced desorption experiment an almost thermal mean kinetic energy of the

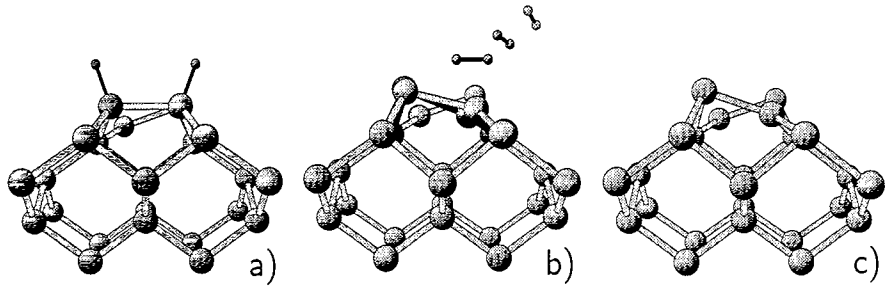

Fig. 16. (a) Hydrogen covered Si(1 0 0) surface (monohydride). (b) Snapshots of a trajectory of D_2 desorbing from Si(1 0 0) starting at the transition state with the Si atoms initial at rest [58]. The dark Si atoms correspond to the Si positions after the desorption event. (c) Clean anti-buckled Si(1 0 0) surface.

molecules was found [190] indicating a low adsorption barrier. In order to explain this puzzle it was suggested to take the strong surface rearrangement of Si upon hydrogen adsorption into account [190]: The hydrogen molecules impinging on the Si substrate from the gas phase typically encounter a Si configuration which is unfavorable for dissociation, while desorbing hydrogen molecules leave the surface from a rearranged Si configuration with a low barrier. In the adsorption process such a surface rearrangement can only be achieved by thermal excitations of the lattice since due to the mass mismatch the silicon substrate atoms are too inert to change their configuration during the time the hydrogen molecule interacts with the surface. The strong surface rearrangement of Si(1 0 0) upon hydrogen adsorption/desorption is illustrated in Fig. 16.

With the assumption of a lattice rearrangement energy of about 0.7 eV existing experimental adsorption and desorption results could be reproduced by quantum dynamical model calculations [9,191,192]. The predicted strong dependence of the adsorption probability on the surface temperature was later confirmed experimentally [188].

So far the dissociation mechanism seemed to be at least qualitatively understood. However, there are some disturbing experimental uncertainties. Measurements of the dissociative adsorption probability of H_2/Si(1 0 0) differ by almost three orders of magnitude from each other [187,189]. In order to explain the large difference it had been speculated [189], e.g., that the Si sample used for the adsorption study of Ref. [187] exhibits an unusual low barrier due to its high dopand concentration of $n \approx 10^{19}$ cm^{-3}.

From the theoretical point of view, the situation is even more confusing. The exact adsorption and desorption mechanism is strongly debated. Total-energy calculations using the cluster approach [193–198] have found activation barriers for associative desorption of hydrogen from Si(1 0 0) which are roughly 1 eV larger than the experimentally found value of about 2.5 eV [183,184]. Based on these findings, the prepairing mechanism has been disregarded, and defect-mediated desorption mechanisms had been proposed [193,195–200]. These mechanisms, however, have difficulties explaining the observed first-order desorption kinetics and the measured high prefactor of the desorption rate (for a thorough discussion of these calculations, see the review by Doren [91]). The question arises whether a cluster really represents a good model for an infinite substrate. For example, in most of the cluster calculations the Si(1 0 0) surface was found to reconstruct with a symmetric dimer structure [195,205,206] while in slab calculations the anti-symmetric buckled dimer structure is the lowest energy configuration [202,203] which is also well-established experimentally [204–206]. It was suggested that the relaxation constraints used in the cluster studies do not model the Si(1 0 0) surface

correctly [207]. Furthermore, the reported barriers for the *same* process differ by almost 1 eV between three different sets of cluster calculations [193–195] indicating the difficulty of such calculations.

On the other hand, in detailed DFT-GGA calculations of the H_2/Si(1 0 0) potential energy surface (PES) using the supercell approach [208–211] and also in cluster calculations [212] desorption barriers for hydrogen atoms originating from the same Si dimer were obtained that are in agreement with the experimentally determined values. This pre-pairing mechanism, as mentioned above, is consistent with the observed first-order kinetics in experiment [182–185]. The adsorption barriers were found to be about 0.3–0.4 eV with the substrate rearrangement energy being roughly 0.15 eV. These barrier heights are also controversely discussed. It was argued that the GGA-PW91 functional used in the DFT studies underestimates the H_2 elimination barriers from silanes, i.e., small molecules [87]. It is, however, questionable whether the results for small molecules are directly transferable to surface systems.

Subsequently, based on the information from the slab calculations [208,209] two different three-dimensional quantum dynamical studies were performed [213,214], where the relaxation of the Si substrate upon hydrogen adsorption was approximated by one idealized Si phonon coordinate. Although both calculations used the same ab initio energies as a source, the results of the dynamical calculations did not agree quantitatively. However, in both studies the dynamical coupling of the desorption path to the Si substrate was low, i.e., the desorbing molecules had more excess translational energy than found in the experiment [190].

These different uncertainties together with the observed unusual first-order desorption kinetics make the H_2/Si(1 0 0) system to one of the most controversely discussed systems in the field of gas–surface dynamics. Since barrier calculations alone will not settle the controversy about the desorption mechanism [91], dynamics calculations are necessary in order to find out how the potential energy at the barrier is distributed over the various degrees of freedom of this system (hydrogen vibration, rotation, and translational energy, and vibrations of the Si substrate). Due to the importance of lattice relaxation effects on the desorption dynamics, substrate degrees of freedom have to be taken into account in the dynamics simulations. This makes a full quantum dynamical treatment not possible at the moment. Ab initio molecular dynamics calculations using both the supercell approach [58] and clusters [59] have therefore been performed. In the supercell calculations DFT-GGA was employed to determine the desorption dynamics of deuterium desorbing from the monohydride (MH) state using a (2×2) surface unit cell and a five-layer Si slab [58] (see Fig. 16). In the cluster calculations hydrogen desorption was treated on the complete active space self-consistent field (CASSCF) level. Both desorption from a single monohydride using a $Si_9\bar{H}_{12}H_2$ cluster and from an isolated dihydride (ID) using a $Si_{10}\bar{H}_{14}H_2$ cluster were studied [59], where $\bar{H}$ denotes the modified hydrogen atoms terminating the cluster.

Since the barrier to associative desorption of hydrogen from Si(1 0 0) is rather high, in both sets of ab initio molecular dynamics calculations [58,59] the trajectories were not started with the hydrogen at the atomic adsorption positions. Instead, the molecular dynamics calculations were initialized with the hydrogen atoms close to the transition state, with initial velocity distributions that correspond to the surface temperatures used in the experiments. In the supercell calculations, additionally the time-reversed trajectories starting at the transition state were determined in order to make sure that all trajectories correspond indeed to desorption and not to scattering events [58].

In the DFT-GGA calculations additional trajectories were determined with the Si lattice initially at rest, i.e., at a surface temperature of $T_s = 0$ K. Snapshots of such a calculated trajectory are shown in Fig. 16(b). The dark Si atoms correspond to the relaxation of the Si lattice after the desorption event.

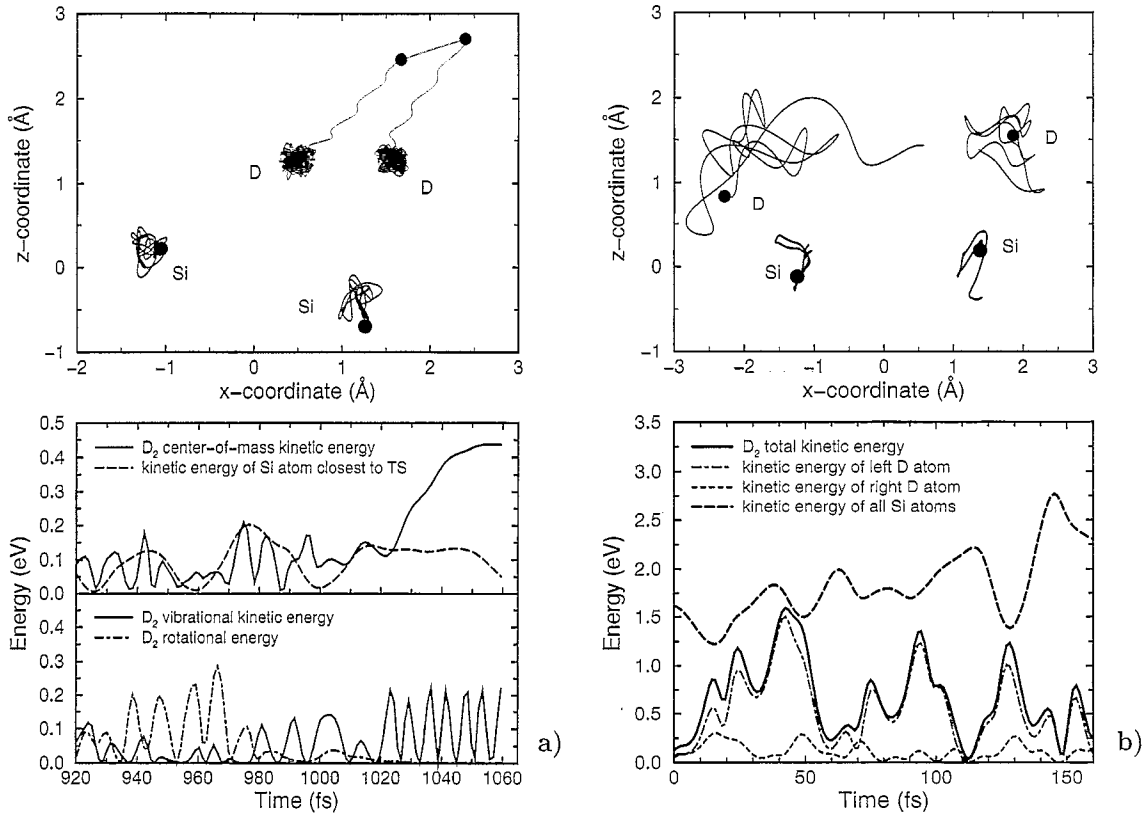

Fig. 17. Ab initio molecular dynamics trajectory of D_2 desorbing from Si(1 0 0). The initial conditions correspond to a surface temperature of $T_S = 920$ K. (a) Thermal desorption trajectory started close to the transition state (TS). Upper panel: x and z coordinates of the trajectories of the two deuterium atoms and the two Si atoms of the dimer underneath the TS. The final positions of the atoms are marked by the large dots. Lower panel: energy redistribution as a function of the last 140 fs of the run-time of the trajectory. The different energy channels are described in the legend of the figure. (b) Time-reversed trajectory of the desorption event started at the TS. The upper and lower panels correspond to the ones in (a).

Approximately 0.1 eV of the potential energy at the transition state is transferred to vibrations of the Si lattice which is a rather large amount compared to hydrogen/metal systems. At the transition state the interatomic hydrogen distance is about 40% larger than the gas-phase bond length; consequently molecular vibrations are excited during the desorption, as is well known for a long time in associative desorption studies (see, e.g., [38]).

Similar results have been found in the DFT-GGA calculations for initial conditions corresponding to a surface temperature of $T_S = 920$ K. In total 34 "thermal" desorption trajectories were calculated. Fig. 17(a) shows an example of such a trajectory. First the surface was equilibrated for approximately 1 ps with the deuterium atoms kept close to the transition state by an auxiliary potential. Then the extra potential was switched off, the molecule was allowed to desorb and the distribution of the energy into the various degrees of freeedom was monitored.

The projection of the trajectories of the desorbing deuterium molecule and of the Si dimer closest to the transition state onto the xz-plane is shown in Fig. 17(a). Due to the asymmetry of the transition state

the molecule does not desorb in the direction normal to the surface. The oscillations in the trajectories correspond to the vibrational excitation of the desorbing D_2. In addition, the energy redistribution during the last 140 fs of the run is plotted where, e.g., the vibrational excitation can be clearly followed. The quenching of the rotational motion is evident which is caused by the strong anisotropy of the PES. Furthermore, the deuterium molecule is strongly accelerated during the desorption event and ends up with a kinetic energy of roughly 0.4 eV which is larger than the value of $2k_BT_s = 0.16$ eV expected for thermal equilibrium.

The configuration at which the extra potential was switched off was also used to start a time-reversed trajectory. As mentioned above, the main reason was to check whether the trajectory describes a true reactive event. On the other hand, the time-reversed trajectory simultaneously corresponds to a dissociative adsorption event and allows us to follow the energy distribution during the adsorption. Once the molecule has passed the transition state, the single atoms are strongly accelerated towards their atomic adsorption positions; together they can gain an energy of 2.5 eV. Fig. 17(b) shows that indeed the two D atoms first become very fast, in particular the left deuterium atom that has the longer distance to its adsorption position. Within 50 fs the D atoms have gained about 1.5 eV in kinetic energy. Although the mass mismatch between the deuterium and the silicon atoms is so large, there is still a significant energy transfer to the silicon lattice due to the high kinetic energy of the D atoms. They bounce into the lattice so violently that within 150 fs 1 eV of the kinetic energy is transferred to the silicon atoms, as Fig. 17(b) reveals. Furthermore, Fig. 17 nicely demonstrates how the atoms of the Si dimer are moving towards a symmetric configuration in the case of the D_2 dissociative adsorption, while in the case of the associative desorption the buckling angle is further increased with respect to the transition state configuration.

The mean total, kinetic, vibrational, and rotational energies and final angles of the hydrogen molecules desorbing from Si(1 0 0) obtained from the ab initio molecular dynamics studies are compared to the experimental results in Table 2. Since there is apparently some confusion about doing a reasonable comparison between theory and experiment, I will briefly expound on the given values. The vibrational and rotational population of hydrogen molecules desorbing from Si(1 0 0) was measured state-specifically using resonance-enhanced multiphonon ionization detection [215]. This gives information about the population of the quantum mechanical eigenstates of the hydrogen molecule. For example, it has been measured that at a surface temperature of $T_s = 780$ K 1% of desorbing H_2 molecules are in the first vibrational eigenstate [215]. This corresponds to a fraction that is 20 times larger than expected in thermal equilibrium and is described by the term "vibrational heating". In [59] this population was used to determine the mean vibrational energy of desorbing H_2 molecules. They obtained a value of 0.264 eV. However, 98% of this value comes from the zero-point energy of the ground-state molecules, only 2% from molecules in the first excited vibrational state. Had the experiments not given any vibrational heating, this mean vibrational energy would have hardly been changed at all. In the ab initio molecular dynamics calculations the dynamics of the hydrogen nuclei is treated fully classically, there are no zero-point energies considered. Since the H_2 zero-point energy is so large (three times larger than the thermal energies in the experiment) it makes no sense comparing a value derived from a quantum mechanical analysis with a classically obtained value. Therefore I have put in Table 2 for the experimental mean vibrational energy the value $\langle E_{vib}\rangle^{exp} = k_BT_{vib}$, where $T_{vib} = 1700$ K was taken from the measured population [215]. This procedure is also not ideal, but certainly closer to a classical analysis. A real quantitative comparison between experiment and theory can only be done for a quantum treatment of the hydrogen vibrational dynamics. In the three-

Table 2
Mean energy distribution and final desorption angle of hydrogen molecules desorbing from a Si(1 0 0) surface

	$\langle E_{tot} \rangle$	$\langle E_{kin} \rangle$	$\langle E_{vib} \rangle$	$\langle E_{rot} \rangle$	$\langle \theta_f \rangle$
D_2, MH, DFT-GGA	0.70 ± 0.18	0.55 ± 0.14	0.12 ± 0.09	0.03 ± 0.05	39.6° ± 10.1°
H_2, MH, CASSCF	0.72 ± 0.20	0.6 ± 0.1	0.09 ± 0.08	0.03 ± 0.02	56° ± 7°
H_2, ID, CASSCF	0.94 ± 0.20	0.7 ± 0.1	0.2 ± 0.1	0.04 ± 0.03	43° ± 17°
D_2, Experiment	0.34 ± 0.05	0.17 ± 0.03	0.15 ± 0.03	0.03 ± 0.01	28° − 31°

The results of the DFT-GGA calculations are averaged over 34 desorption trajectories corresponding to D_2 desorption from the monohydride (MH) phase at a surface temperature of $T_s = 920\,K$ ($k_B T_s = 0.079\,eV$) [58]. The cluster calculations at the CASSCF level for H_2 desorption from a MH and an isolated dihydride (ID) are averaged over 10 trajectories for each case at a surface temperature of $T_s = 780\,K$ ($k_B T_s = 0.067\,eV$) [59]. The experimental results are collected from [56]. The translational energy has been been determined in a laser-induced desorption experiment where the surface temperature was estimated to be $T_s = 920\,K$ [190] while the vibrational and rotational energy have been measured at a surface temperature of $T_s = 780$ K [215]. The mean vibrational energy corresponds to the classical value using the vibrational temperature measured in the experiment (see text). The experimental mean desorption angles are derived from [216], where the angular distribution in desorption has been measured for two different hydrogen coverages.

dimensional quantum dynamical studies, e.g, the correct experimental population of vibrationally excited states in desorption is reproduced [191,192,213]. These problems do not arise for the mean translational and rotational energies. Since these modes are free in the gas-phase, there are no zero-point energies associated with them.

Furthermore, in [59] a mean experimental kinetic energy of 0.34 eV for H_2 desorption was derived which was said to be scaled from the experimental value of 0.17 eV for D_2. This scaling seems very questionable to me. H_2 and D_2 have exactly the same interaction potential. The gain in kinetic energy is determined by the change in the potential energy which is the same for H_2 and D_2. And classically different isotopes follow exactly the same trajectories as a function of the kinetic energy if no energy transfer to substrate degrees of freedom is considered [51]. Hence H_2 and D_2 should have approximately the same kinetic energy in desorption. There can be an isotope effect due to quantum mechanical effects or due to energy transfer to the silicon lattice. However, the sign and magnitude of this isotope effect is not clear a priori; it has to be determined by detailed calculations. Certainly it does not follow such a simple scaling law as assumed in [59].

Comparing the theoretical and experimental data in Table 2, it should furthermore be noted that the reported theoretical values do not really correspond to any thermal average. For that purpose the number of 34 and 10 calculated trajectories, respectively, is much too low. Hence the theoretical results have to be interpreted cautiously. Still they should be able to indicate the general trends in the energy distribution of desorbing molecules since in thermal desorption the molecules mainly originate from a small fraction of the configuration space close to the transition state (the so-called keyhole effect [26]). As for the mean desorption angle, note that this value correspond to an average over all azimuthal angles with $0 \leq \theta_f < 90°$. Hence even if the angular distribution for fixed azimuth is peaked in the direction normal to the surface, $\langle \theta_f \rangle$ will still be larger than zero.

It is obvious that all simulations reproduce the vibrational heating, i.e. $\langle E_{vib} \rangle > k_B T_s$, and the rotational cooling, i.e. $\langle E_{rot} \rangle < k_B T_s$. The final desorption angles are slightly larger than the experimental result [216]. The mean kinetic energy, however, is much larger for all ab initio molecular dynamics calculations than the experimental value for D_2 of $\langle E_{kin} \rangle^{exp} = 0.17$ eV $2k_B T_s$ [190]. In the

cluster calculations, molecules desorbing from the isolated dihydride are even faster than molecules desorbing from the monohydride. It is remarkable that the results of the supercell and the cluster calculations are rather similar for the mean final energies of hydrogen molecules desorbing from the monohydride state.

The theoretical mean desorption angles are somewhat larger than the experimental values. However, due to the low number of trajectories obtained in the calculations the discrepancies are not conclusive to rule out any particular mechanism.

In conclusion, the analysis of the data of Table 2 gives no reason to disregard the prepairing mechanism with respect to any defect-mediated mechanism. According to the results of the ab initio molecular dynamics runs [59], the isolated dihydride mechanism does even worse compared to the experiment than does the prepairing mechanism. Since the observed first-order kinetics in hydrogen desorption from Si(1 0 0) follows very naturally from the prepairing process, this still seems to be the most probable mechanism of desorption. Just recently there has been a very detailed temperature programmed desorption study of hydrogen desorption from Si(1 0 0) at low coverages which gave no indication that defect sites are involved in the desorption process [217]. Similar conclusions can be drawn from another recent study about hydrogen adsorption on Si(1 0 0) which allowed a discrimination between hydrogen adsorption on step and defect sites and on terrace sites [218].

The question still remains why the kinetic energy in desorption comes out much larger in the ab initio molecular dynamics runs than in the experiment. Uncertainties due to the bad statistics of the molecular dynamics runs or quantum dynamical effects are not believed to be responsible for the large difference [58,214]. In all the ab initio calculations the electrons are assumed to follow the motion of the nuclei adiabatically in their ground state. It has therefore been speculated that the excess energy at the transition state might be transferred to surface electronic excitations [58,91] thus taking energy away from the molecular degrees of freedom. Besides, the laser-induced desorption used in the experiment to determine the translational energy in desorption [190] might not correspond to thermal desorption events described by the ab initio molecular dynamics runs. Recent DFT calculations indicate that laser melting of bulk silicon leads to a transition to a metallic liquid state [219] which could also occur during the laser-induced desorption used in the experiment. Furthermore, at surface temperatures above 900 K the clean Si(1 0 0) surface undergoes a semiconductor–metal transition [220]. At a metallic surface the barrier distribution might be different. In addition, the excitation of electron–hole pairs is much more probable leading to an effective dissipation channel for any excess energy at the transition state. Since all these considerations about the correct desorption mechanism rely on *one* laser-induced desorption experiment, it is highly desirable that the mean kinetic energy of hydrogen molecules desorbing from Si(1 0 0) is measured independently by preferentially a thermal desorption experiment.

4.2. Reactions of atomic hydrogen with hydrogen-passivated semiconductor surfaces

The associative desorption reaction described in the previous section is of the so-called Langmuir–Hinshelwood (LH) type in which both reactants are equilibrated with the substrate before the reaction. In the Eley–Rideal mechanism, on the other hand, an incoming gas-phase species is assumed to react directly with an adsorbate and abstract it from the surface. In Fig. 18 such an abstraction reaction is illustrated. Since in the ER reaction mechanism only one atom–surface bond has to be broken instead of two in the LH mechanism, the ER reactions show a significant exothermicity leading to large translational and internal energies in the desorbing products. Although the concept has long been

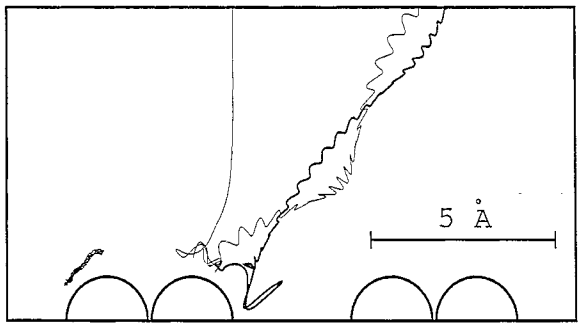

Fig. 18. Example of a reactive trajectory for a H atom abstracting a D atom adsorbed on Si(1 0 0). The incident kinetic energy of the H atom is 0.2 eV (from [229]).

known, experimentally the Eley–Rideal mechanism has only recently been confirmed, at first for hydrogen abstraction reactions from metal surfaces [221–224]. In the meantime also hydrogen abstraction reactions from Si surfaces have been observed [225,226]. These abstraction reactions have been found to be very efficient: the reaction probability for abstraction on the saturated monohydride surface is 0.5 ± 0.1 relative to the atomic adsorption probability on the clean surface [225]. Since the adsorption probability of hydrogen atoms on Si surfaces is of order unity [227], this means that roughly half of the incoming molecules pick up another hydrogen atom from the surface. However, only a small fraction of the incoming atoms directly hit the adsorbed hydrogen atoms. In order to explain the observed adsorption kinetics and the high abstraction probability, it was therefore suggested that also indirect processes take place [225]. The impinging atom does not immediately pick up another atom from the surface but remains trapped at the surface while keeping most of its energy before the abstraction reaction. This mechanism, which has also been suggested for hydrogen abstraction reactions on metal surfaces [228], is called "hot precursor" [225] or "hot atom" [229] mechanism and has first been addressed by Harris and Kasemo [230].

Theoretically ER reactions have first been treated by low-dimensional quantum model studies in restricted geometries [118,231,232]. These studies focused on the strong vibrational excitation of the molecules upon the abstraction reaction. Such a low-dimensional treatment does not allow the description of the hot atom process. In order to figure out the importance of these indirect processes, it is still unavoidable to rather perform classical dynamical calculations with a high dimensionality instead of quantum calculations with a restricted dimensionality. However, this is a reasonable approach since due to the large exothermicity of the reaction quantum effects should be negligible. Classical trajectory calculations of the reaction dynamics of atomic hydrogen with the hydrogenated Si(1 0 0) surface have recently been performed by Kratzer [62,229]. In these studies the PES has been described in a modified LEPS form. The energy transfer to the Si substrate is taken into account by a collective mode in the surface oscillator model. In a first study, the LEPS parameters were derived from both experiment and ab initio calculations [229]. In a subsequent treatment the PES parameters were all obtained by spin-polarized DFT-GGA calculations in the supercell approach [62].

Fig. 18 shows an example of a calculated reactive trajectory. An incoming H atom is directly abstracting an adsorbed D atom. The fast oscillations illustrate the strong vibrational excitation of the product HD molecule while the slow oscillations correspond to the rotational excitation. However, such a direct ER reaction is in fact less probable than an indirect hot atom abstraction reaction, as the

ab initio molecular dynamics calculations reveal [62]. For H atoms incident with kinetic energies above 1 eV less than 20% of the produced HD molecules originate from direct ER reactions.

Briefly summarizing the theoretical results, it is found that the abstraction probability, which agrees with the experiment within the experimental uncertainty, decreases with increasing incident kinetic energy. Most of the energy dissipated to the surface is transferred to vibrations of the adsorbed hydrogens remaining on the surface since the energy transfer to the Si substrate atoms is rather low due to the large mass mismatch between H and Si. But the most important channel of energy disposal in the reaction is the kinetic energy of the hydrogen molecules. Just recently also the H absorption in and adsorption on Cu(111) has been studied by molecular dynamics calculations where the PES was derived from DFT calculations and expanded in an effective-medium theory form [233]. These calculations confirm that ab initio molecular dynamics studies are an indispensable tool to complement experimental information, since contrary to the experiment the calculations allow a microscopic analysis of the reaction dynamics.

5. Laser-induced desorption

So far all reported ab initio dynamics studies employed the Born–Oppenheimer approximation, i.e., the electrons were assumed to follow the motion of the nuclei adiabatically. However, one very active field of experimental research during the last years has been the study of desorption induced by electronic transitions, so-called DIET processes [234]. These processes can either be induced by electron impact (ESD) or by light (PSD). The abbreviations denote electron or photon stimulated desorption, respectively. In particular, there have been numerous investigations of laser-induced desorption of small molecules from surfaces (for a review, see [235]).

The theoretical description of the dynamics of desorption processes involving electronically excited states is rather complex. In most studies the electron dynamics is not taken into account explicitly, instead the electronic transitions are treated in the Frank–Condon or sudden approximation [236,237]. In a quantum treatment of the dynamics of the nuclei this corresponds to the jumping of wave packets between different electronic states of the molecule–surface system. Usually only the electronic ground state and one excited state are considered. In these studies the total energy is not conserved, i.e., it is assumed that the energy difference between the electronic states is entirely taken away by the electrons. To overcome this problem, either the electron dynamics have to be treated explicitly [238] or the excitation spectrum of the solid has to be taken into account [239].

Although the modeling of laser-induced desorption can be rather successful in elucidating dynamical aspects of the processes (see, e.g., [240,241]), the potential curves for the electronic excited states had to be guessed since there were no accurate calculations for them. Furthermore, at metal surfaces the electronically excited states are strongly coupled to the continuous electronic excitation spectrum of the surface. It is questionable whether the description of a DIET process with just one sharp well-defined electronically excited state is reasonable in this strong-coupling regime.

This situation is different for the excited states at insulator surfaces like oxides due to the large band gap. In addition, due to the strong ionicity of these systems a local description of the electronic structure is reasonable. This is important insofar as density functional theory is an electronic ground state theory and does not straightforwardly allow the determination of excited state potentials (there are DFT calculations describing electronic excited states, though, see for example [92]). Hence one has to

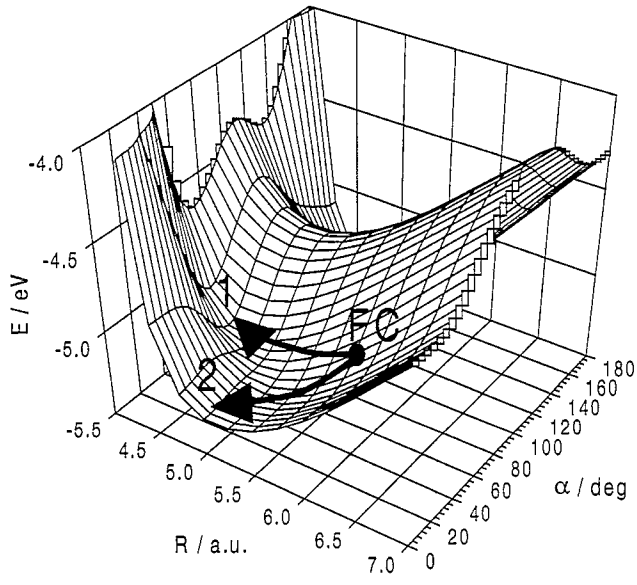

Fig. 19. Charge transfer PES of NO/NiO(1 0 0) as a function of the NO center of mass distance R from the surface and the polar orientation of the molecule α. FC denotes the Franck–Condon point at which the wave-packet propagation is started (from [69]).

employ quantum chemical ab initio methods which require the use of a cluster approach. Indeed such an approach has been followed recently for the first time. Klüner and coworkers have performed configuration interaction (CI) calculations for the construction of potential energy surfaces for electronically excited states describing the laser-induced desorption of NO from NiO(1 0 0) [68,69,242]. In the CI calculations a NiO_5^{8-} cluster was embedded in a semi-infinite Madelung potential of ± 2 point charges for the simulation of the NiO(1 0 0) surface. The calculated ground state potential did in fact not reproduce the experimentally found binding energy of 0.52 eV [243], confirming the well-known problems in determining binding energies at surfaces by cluster calculations [80]. The ab initio minimum has therefore been scaled to fit the experimental data [69]. One specific charge transfer state in which one electron was transferred from the cluster to the NO molecule was used as a representative electronically excited state. The potential energy surfaces were determined as a function of the NO center of mass distance from the surface and the polar orientation of the molecule with respect to the surface normal. Fig. 19 shows the excited state potential.

The dynamics of the laser-induced desorption of NO from NiO(1 0 0) were simulated by the jumping wave packet method in which the molecular distance from the surface and the polar and azimuthal orientation of the molecule were considered explicitly. The laser-induced electronic excitation was modeled by putting the three-dimensional ground state wave function of the electronic ground state onto the electronically excited PES. Thereby the center of the wave function is located at the Franck–Condon point FC shown in Fig. 19. The minimum of the excited state potential is closer to the surface than in the ground state potential leading to an acceleration of the wave packet towards the surface. This is called an Antoniewicz desorption scenario [244]. The wave packet is then propagated for a certain residence time on the excited state potential before it is transferred in a second Franck–Condon

transition back to the electronic ground state. Molecules that have gained enough kinetic energy after the Franck–Condon transitions are able to desorb. The finite residence time is due to the interaction of the excited state with the electronic spectrum of the substrate. The coupling strength of this interaction that causes the quenching of the electronic excitation is still unknown. Hence the mean residence time, the so-called *resonance* time τ_r, enters as an adjustable parameter in the dynamics simulation. A value of $\tau_r = 24$ fs has been chosen which yields a desorption probability of 3.3% in agreement with typical experimental data [69,245].

Since the wave packet calculations are performed within a restricted dimensionality, quantitative agreement with the experiment [245] cannot be the ultimate goal of this theoretical study. More important is to gain a qualitative understanding of experimental trends. Indeed this study provides such a qualitative concept. The excited state potential has a complicated shape as a function of the polar orientation of the molecule. Two possible pathways are sketched in Fig. 19 along which partial wave packets can propagate. This bifurcation of the wave packet causes a bimodality in the calculated velocity distribution of desorbing molecules. This bimodality has also been found in the experiment [245]. Hence the ab initio treatment of the laser-induced desorption relates qualitative trends in the experimental results to microscopic details of the potential energy surfaces.

6. Conclusions and outlook

In this review ab initio dynamics studies of reactions on surfaces have been presented. In the last years the interaction between electronic structure calculations on the one side and dynamical calculations on the other side has been very fruitful. The availability of high-dimensional reliable potential energy surfaces has challenged the dynamics community to improve their methods in order to perform high-dimensional dynamical studies on these potentials. Now quantum studies of the dissociation of hydrogen on surfaces are possible in which all six degrees of freedom of the molecule are treated dynamically. In this review I have tried to show that this achievement represents an important step forward in our understanding of the interaction of molecules with surfaces. Not only the quantitative agreement with experiment is improved, but also important qualitative concepts emerge from these high-dimensional calculations.

However, what are the next steps to be taken in the application of ab initio dynamics studies? The six-dimensional dynamical treatment of hydrogen dissociation represents the achievement of a goal that has long been pursued. But due to the unfavorable scaling of the quantum dynamical methods with the number of channels there will probably be no seven- or eight-dimensional quantum calculations in the near future (although there are nevertheless some promising approaches [246]). Neither will there soon be a six-dimensional quantum treatment of molecules heavier than hydrogen for the same reason. But for these heavier molecules quantum effects are not so important so that a classical treatment of the dynamics will be sufficient.

The important class of oxidation reactions, for example, will certainly soon be the subject of ab initio studies in which the dynamics is treated classically. In ab initio molecular dynamics simulation also the energy transfer to substrate phonons can be taken into account by explicitly including the upper layers of the surface in the trajectory calculations. Still the quantum treatment of dissipation is an important goal because it would allow the energy transfer to phonons and to electron–hole pairs to be treated on an equal footing. This issue leads over to the treatment of electronically non-adiabatic processes. In this

important field both the determination of excited state potentials as well as the description of non-adiabatic dynamics still represent a great challenge where much progress has to be made.

Finally it should be mentioned that there is still room for low-dimensional model studies. In order to find out how the reaction dynamics depends on specific details of the PES, it is usually very instructive to perform dynamical simulations in which certain features of the PES are changed in a controlled fashion within a restricted dimensionality. However, without any ab initio calculations it is often impossible to even guess the general shape of the PES for a more complicated reaction. This confirms the important role that ab initio dynamics calculations play for the advancement of our understanding of reactions on surfaces, even for model studies.

Acknowledgements

I am very grateful to all my collegues and coworkers who have contributed to the results presented in this review. I would like to mention Michel Bockstedte, Thomas Brunner, Bjørk Hammer, Peter Kratzer, Eckhard Pehlke, Ralf Russ, Ching-Ming Wei, Steffen Wilke, and my supervisors Helmar Teichler, Wilhelm Brenig and Matthias Scheffler. In particular, without the discussions and the close ongoing collaboration with Wilhelm Brenig and Matthias Scheffler this work would have been impossible. I would also like to thank them and Peter Kratzer and Paolo Ruggerone for their critical reading of the manuscript. Special thanks go to Peter Kratzer and Thorsten Klüner for sharing their results with me prior to publication.

References

[1] A. Zangwill, Physics at Surfaces, Cambridge University Press, Cambridge, 1988.
[2] M.C. Desjonquéres, D. Spanjaard, Concepts in Surface Physics, 2nd ed., Springer, Berlin, 1996.
[3] B. Jackson, H. Metiu, J. Chem. Phys. 86 (1987) 1026.
[4] D. Halstead, S. Holloway, J. Chem. Phys. 93 (1990) 2859.
[5] G.R. Darling, S. Holloway, J. Chem. Phys. 97 (1992) 734.
[6] S. Küchenhoff, W. Brenig, Y. Chiba, Surf. Sci. 245 (1991) 389.
[7] L. Schröter, S. Küchenhoff, R. David, W. Brenig, H. Zacharias, Surf. Sci. 261 (1992) 243.
[8] G.R. Darling, S. Holloway, Surf. Sci. 268 (1992) L305.
[9] W. Brenig, A. Gross, R. Russ, Z. Phys. B 96 (1994) 231.
[10] M. Hand, J. Harris, J. Chem. Phys. 92 (1990) 7610.
[11] A. Gross, Surf. Sci. 320 (1994) L68.
[12] G.R. Darling, S. Holloway, Surf. Sci. 321 (1994) L189.
[13] R.C. Mowrey, J. Chem. Phys. 99 (1993) 7049.
[14] G.R. Darling, S. Holloway, J. Chem. Phys. 101 (1994) 3268.
[15] T. Brunner, W. Brenig, Surf. Sci. 317 (1994) 303.
[16] J. Dai, J.Z.H. Zhang, J. Chem. Phys. 102 (1995) 6280.
[17] M. Karikorpi, S. Holloway, N. Henriksen, J.K. Nørskov, Surf. Sci. 179 (1987) L41.
[18] U. Nielsen, D. Halstead, S. Holloway, J.K. Nørskov, J. Chem. Phys. 93 (1990) 2879.
[19] D. Halstead, S. Holloway, J. Chem. Phys. 88 (1988) 7197.
[20] G.R. Darling, S. Holloway, J. Chem. Phys. 93 (1990) 9145.
[21] G.R. Darling, S. Holloway, J. Chem. Phys. 97 (1992) 5182.
[22] G.R. Darling, S. Holloway, Surf. Sci. 304 (1994) L461.

[23] A. Gross, W. Brenig, Chem. Phys. 177 (1993) 497.
[24] A. Gross, W. Brenig, Surf. Sci. 289 (1993) 335.
[25] A. Gross, W. Brenig, Surf. Sci. 302 (1994) 403.
[26] A. Gross, J. Chem. Phys. 102 (1995) 5045.
[27] W.A. Diño, H. Kasai, A. Okiji, Phys. Rev. Lett. 78 (1997) 286.
[28] A. Kara, A.E. DePristo, J. Chem. Phys. 92 (1990) 5653.
[29] K. Yang, T.S. Rahman, J. Chem. Phys. 93 (1990) 6834.
[30] C. Engdahl, U. Nielsen, Chem. Phys. Lett. 215 (1993) 103.
[31] C. Engdahl, B.I. Lundqvist, U. Nielsen, J.K. Nørskov, Phys. Rev. B 45 (1992) 11362.
[32] C. Engdahl, U. Nielsen, J. Chem. Phys. 98 (1993) 4223.
[33] A. Grüneich, A.J. Cruz, B. Jackson, J. Chem. Phys. 98 (1993) 5800.
[34] S. Kumar, B. Jackson, J. Chem. Phys. 100 (1994) 5956.
[35] A.E. DePristo, A. Kara, Adv. Chem. Phys. 77 (1991) 163.
[36] S. Holloway, Surf. Sci. 299/300 (1994) 656.
[37] J.C. Tully, Surf. Sci. 299/300 (1994) 667.
[38] G.R. Darling, S. Holloway, Rep. Prog. Phys. 58 (1995) 1595.
[39] B. Hammer, M. Scheffler, K.W. Jacobsen, J.K. Nørskov, Phys. Rev. Lett. 73 (1994) 1400.
[40] J.A. White, D.M. Bird, M.C. Payne, I. Stich, Phys. Rev. Lett. 73 (1994) 1404.
[41] S. Wilke, M. Scheffler, Surf. Sci. 329 (1995) L605.
[42] S. Wilke, M. Scheffler, Phys. Rev. B 53 (1996) 4926.
[43] S. Wilke, M. Scheffler, Phys. Rev. Lett. 76 (1996) 3380.
[44] C.M. Wei, A. Gross, M. Scheffler, Phys. Rev. B 57 (1998) 15572.
[45] B. Hammer, M. Scheffler, Phys. Rev. Lett. 74 (1995) 3487.
[46] J.A. White, D.M. Bird, M.C. Payne, Phys. Rev. B 53 (1996) 1667.
[47] G. Wiesenekker, G.J. Kroes, E.J. Baerends, J. Chem. Phys. 104 (1996) 7344.
[48] A. Eichler, G. Kresse, J. Hafner, Phys. Rev. Lett. 77 (1996) 1119.
[49] W. Dong, J. Hafner, Phys. Rev. B 56 (1996) 15396.
[50] A. Gross, S. Wilke, M. Scheffler, Phys. Rev. Lett. 75 (1995) 2718.
[51] A. Gross, M. Scheffler, Phys. Rev. B 57 (1998) 2493.
[52] G.J. Kroes, E.J. Baerends, R.C. Mowrey, Phys. Rev. Lett. 78 (1997) 3583.
[53] G.J. Kroes, E.J. Baerends, R.C. Mowrey, J. Chem. Phys. 107 (1997) 3309.
[54] H. Hellmann, Einführung in die Quantenchemie, Deuieke, Leipzig, 1937, p. 285.
[55] R.P. Feynman, Phys. Rev. 56 (1939) 340.
[56] K.W. Kolasinski, Int. J. Modern Phys. B 9 (1995) 2753.
[57] A. De Vita, I. Štich, M.J. Gillan, M.C. Payne, L.J. Clarke, Phys. Rev. Lett. 71 (1993) 1276.
[58] A. Gross, M. Bockstedte, M. Scheffler, Phys. Rev. Lett. 79 (1997) 701.
[59] A.J.R. da Silva, M.R. Radeke, E.A. Carter, Surf. Sci. 381 (1997) L628.
[60] M.R. Radeke, E.A. Carter, Annu. Rev. Phys. Chem. 48 (1997) 243.
[61] M. Kay, G.R. Darling, S. Holloway, J.A. White, D.M. Bird, Chem. Phys. Lett. 245 (1995) 311.
[62] P. Kratzer, Chem. Phys. Lett. 288 (1998) 396.
[63] A. Eichler, J. Hafner, Phys. Rev. Lett. 79 (1997) 4481.
[64] P.A. Gravil, D.M. Bird, J.A. White, Phys. Rev. Lett. 77 (1996) 3933.
[65] D.M. Bird, P.A. Gravil, Surf. Sci. 377 (1997) 555.
[66] A. Eichler, Dissertation, Technical University Vienna, 1998.
[67] C. Stampfl, M. Scheffler, Phys. Rev. Lett. 78 (1997) 1500.
[68] T. Klüner, J. Freitag, H.-J. Freund, V. Staemmler, J. Mol. Catal. A 119 (1997) 155.
[69] T. Klüner, H.-J. Freund, V. Staemmler, R. Kosloff, Phys. Rev. Lett. 80 (1998) 5208.
[70] M. Born, J.R. Oppenheimer, Ann. Phys. 84 (1927) 457.
[71] T. Greber, Surf. Sci. Rep. 28 (1997) 1.
[72] M. Born, K. Huang, Dynamical Theory of Crystal Lattices, Clarendon Press, Oxford, 1954, p. 406.
[73] P. Hohenberg, W. Kohn, Phys. Rev. 136 (1964) B864.
[74] W. Kohn, L.J. Sham, Phys. Rev. 140 (1965) A1133.

[75] E.L. Briggs, D.J. Sullivan, J. Bernholc, Phys. Rev. B 54 (1996) 14362.
[76] A. Gross, H. Teichler, Phil. Mag. B 64 (1991) 413.
[77] M. Scheffler, Ch. Droste, A. Fleszar, F. Máca, G. Wachutka, G. Barzel, Physica B 172 (1991) 143.
[78] P.J. Feibelman, Phys. Rev. B 46 (1992) 15416.
[79] M.I. Trioni, G.P. Brivio, S. Crampin, J.E. Inglesfield, Phys. Rev. B 53 (1996) 8052.
[80] J.L. Whitten, H. Yang, Surf. Sci. Rep. 24 (1996) 55.
[81] R.M. Dreizler, E.K.U. Gross, Density Functional Theory, Springer, Berlin 1990.
[82] M.C. Payne, M.P. Teter, D.C. Allan, T.A. Arias, J.D. Joannopoulos, Rev. Modern Phys. 64 (1992) 1045.
[83] A.D. Becke, Phys. Rev. A 38 (1988) 3098.
[84] C. Lee, W. Yang, R.G. Parr, Phys. Rev. B 37 (1988) 785.
[85] J.P. Perdew J.A. Chevary, S.H. Vosko, K.A. Jackson, M.R. Pederson, D.J. Singh, C. Fiolhias, Phys. Rev. B 46 (1992) 6671.
[86] J.P. Perdew, K. Burke, M. Enzerhoff, Phys. Rev. Lett. 77 (1996) 3865.
[87] P. Nachtigall, K.D. Jordan, A. Smith, H. Jónsson, J. Chem. Phys. 104 (1996) 148.
[88] R. Car, M. Parrinello, Phys. Rev. Lett. 55 (1985) 2471.
[89] P Bendt, A. Zunger, Phys. Rev. Lett. 50 (1983) 1684.
[90] B.I. Dunlap, N. Rösch, Adv. Quantum Chem. 21 (1990) 317.
[91] D.J. Doren, Adv. Chem. Phys. 95 (1996) 1.
[92] O. Pankratov, M. Scheffler, Phys. Rev. Lett. 75 (1995) 701.
[93] A. Gross, B. Hammer, M. Scheffler, W. Brenig, Phys. Rev. Lett. 73 (1994) 3121.
[94] A.D. Kinnersley, G.R. Darling, S. Holloway, B. Hammer, Surf. Sci. 364 (1996) 219.
[95] D.E. Makarov, H. Metiu, J. Chem. Phys. 108 (1998) 590.
[96] T.B. Blank, S.D. Brown, A.W. Calhoun, D.J. Doren, J. Chem. Phys. 103 (1995) 4129.
[97] K.T. No, B.H. Chang, S.Y. Kim, M.S. Jhon, H.A. Scheraga, Chem. Phys. Lett. 271 (1997) 152.
[98] S. Lorenz, A. Gross, M. Scheffler, APS Bull. 43 (1998) 235.
[99] M.J. Mehl, D.A. Papaconstantopoulos, Phys. Rev. B 54 (1996) 4519.
[100] G.M. Goringe, D.R. Bowler, E. Hernández, Rep. Progr. Phys. 60 (1997) 1447.
[101] A. Gross, M. Scheffler, M.J. Mehl, D.A. Papaconstantopoulos, submitted.
[102] J.C. Slater, G.F. Koster, Phys. Rev. 94 (1954) 1498.
[103] A. Gross, C.M. Wei, M. Scheffler, Surf. Sci., in press.
[104] R.G. Newton, Scattering Theory of Waves, Particles, 2nd ed., Springer, New York, 1982.
[105] G.L. Hofacker, Z. Naturforsch. 18a (1963) 607.
[106] R.A. Marcus, J. Chem. Phys. 41 (1964) 2614.
[107] W. Brenig, H. Kasai, Surf. Sci. 213 (1989) 170.
[108] W. Brenig, T. Brunner, A. Gross, R. Russ, Z. Phys. B 93 (1993) 91.
[109] Y. Chiba, W. Brenig, Surf. Sci. 306 (1994) 406.
[110] W. Brenig, R. Russ, Surf. Sci. 315 (1994) 195.
[111] W. Brenig, A. Gross, R. Russ, Z. Phys. B 97 (1995) 311.
[112] J.A. Fleck, J.R. Morris, M.D. Feit, Appl. Phys. 10 (1976) 129.
[113] M.D. Feit, J.A. Fleck, A. Steiger, J. Comput. Phys. 47 (1982) 412.
[114] H. Tal-Ezer, R. Kosloff, J. Chem. Phys. 81 (1984) 3967.
[115] W.H. Press, B.P. Flannery, S.A. Teukolsky, W.T. Vetterling, Numerical Recipes, Cambridge University Press, Cambridge, 1989.
[116] J.E. Müller, Phys. Rev. Lett. 59 (1987) 2943.
[117] A.C. Luntz, J. Harris, Surf. Sci. 258 (1991) 397.
[118] P. Kratzer, W. Brenig, Surf. Sci. 254 (1991) 275.
[119] P.J. Feibelman, D.R. Hamann, Phys. Rev. Lett. 52 (1984) 61.
[120] J. Harris, S. Andersen, Phys. Rev. Lett. 55 (1985) 1583.
[121] S. Wilke, M.H. Cohen, M. Scheffler, Phys. Rev. Lett. 77 (1996) 1560.
[122] S. Wilke, Appl. Phys. A 63 (1996) 583.
[123] B. Hammer, J.K. Nørskov, Nature 376 (1995) 238.
[124] B. Hammer, J.K. Nørskov, Surf. Sci. 343 (1995) 211.
[125] C.T. Rettner, D.J. Auerbach, H.A. Michelsen, Phys. Rev. Lett. 68 (1992) 1164.

[126] C.T. Rettner, H.A. Michelsen, D.J. Auerbach, J. Chem. Phys. 102 (1995) 4625.
[127] B.E. Hayden, C.L.A. Lamont, Phys. Rev. Lett. 63 (1989) 1823.
[128] G. Anger, A. Winkler, K.D. Rendulic, Surf. Sci. 220 (1989) 1.
[129] K.D. Rendulic, A. Winkler, Surf. Sci. 299/300 (1994) 261.
[130] P. Kratzer, B. Hammer, J.K. Nørskov, Surf. Sci. 359 (1996) 45.
[131] G. Wiesenekker, G.J. Kroes, E.J. Baerends, R.C. Mowrey, J. Chem. Phys. 102 (1995) 3873.
[132] M. Städele, J.A. Majewski, P. Vogl, A. Görling, Phys. Rev. Lett. 79 (1997) 2089.
[133] J.R. Chelikowsky, M. Schlüter, S.G. Louie, M.L. Cohen, Solid State Commun. 17 (1975) 1103.
[134] H.A. Michelsen, D.J. Auerbach, J. Chem. Phys. 94 (1991) 7502.
[135] A. Eichler, G. Kresse, J. Hafner, Surf. Sci. 397 (1998) 116.
[136] J.C. Polanyi, W.H. Wong, J. Chem. Phys. 51 (1969) 1439.
[137] A. Gross, M. Scheffler, Chem. Phys. Lett. 256 (1996) 417.
[138] M.J. Murphy, A. Hodgson, J. Chem. Phys. 108 (1998) 4199.
[139] J. Dai, J.C. Light, J. Chem. Phys. 107 (1997) 1676.
[140] D. Wetzig, M. Rutkowski, R. David, H. Zacharias, Europhys. Lett. 36 (1996) 31.
[141] S.J. Gulding, A.M. Wodtke, H. Hou, C.T. Rettner, H.A. Michelsen, D.J. Auerbach, J. Chem. Phys. 105 (1996) 9702.
[142] H. Hou, S.J. Gulding, C.T. Rettner, A.M. Wodtke, D.J. Auerbach, Science 277 (1997) 80.
[143] C. Cottrell, R.N. Carter, A. Nesbitt, P. Samson, A. Hodgson, J. Chem. Phys. 106 (1997) 4714.
[144] M.J. Murphy, A. Hodgson, Phys. Rev. Lett. 78 (1997) 4458.
[145] K.D. Rendulic, G. Anger, A. Winkler, Surf. Sci. 208 (1989) 404.
[146] C.T. Rettner, D.J. Auerbach, Chem. Phys. Lett. 253 (1996) 236.
[147] Ch. Resch, H.F. Berger, K.D. Rendulic, E. Bertel, Surf. Sci. 316 (1994) L1105.
[148] H.F. Berger, Ch. Resch, E. Grösslinger, G. Eilmsteiner, A. Winkler, K.D. Rendulic, Surf. Sci. 275 (1992) L627.
[149] D.A. Butler, B.E. Hayden, J.D. Jones, Chem. Phys. Lett. 217 (1994) 423.
[150] P. Alnot, A. Cassuto, D.A. King, Surf. Sci. 215 (1989) 29.
[151] D.A. Butler, B.E. Hayden, Chem. Phys. Lett. 232 (1995) 542.
[152] St.J. Dixon-Warren, A.T. Pasteur, D.A. King, Surf. Rev. Lett. 1 (1994) 593.
[153] D.A. King, CRC Crit. Rev. Solid State Mater. Sci. 7 (1978) 167.
[154] A. Gross, M. Scheffler, Phys. Rev. Lett. 77 (1996) 405.
[155] A. Gross, M. Scheffler, Chem. Phys. Lett. 263 (1996) 567.
[156] S. Holloway, M. Kay, G.R. Darling, Faraday Disc. Chem. Soc. 105 (1996) 209.
[157] C.T. Rettner, D.J. Auerbach, Phys. Rev. Lett. 77 (1996) 404.
[158] C.T. Rettner, H.A. Michelsen, D.J. Auerbach, Chem. Phys. 175 (1993) 157.
[159] A. Gross, M. Scheffler, J. Vac. Sci. Technol. A 15 (1997) 1624.
[160] A. Gross, S. Wilke, M. Scheffler, Surf. Sci. 357/358 (1996) 614.
[161] M. Beutl, M. Riedler, K.D. Rendulic, Chem. Phys. Lett. 247 (1995) 249.
[162] M. Gostein, G.O. Sitz, J. Chem. Phys. 106 (1997) 7378.
[163] M. Beutl, M. Riedler, K.D. Rendulic, Chem. Phys. Lett. 256 (1996) 33.
[164] L. Schröter, R. David, H. Zacharias, Surf. Sci. 258 (1991) 259.
[165] L. Schröter, R. David, H. Zacharias, J. Vac. Sci. Technol. A 9 (1991) 1712.
[166] S. Andersson, J. Harris, Phys. Rev. Lett. 48 (1982) 545.
[167] M. Beutl, K.D. Rendulic, G.R. Castro, Surf. Sci. 385 (1997) 97.
[168] C.H. Greene, R.N. Zare, J. Chem. Phys. 78 (1983) 6741.
[169] D. Wetzig, R. Dopheide, M. Rutkowski, R. David, H. Zacharias, Phys. Rev. Lett. 76 (1996) 463.
[170] A. Gross, M. Scheffler, Prog. Surf. Sci. 53 (1996) 187.
[171] D. Wetzig, M. Rutkowski, W. Etterich, R. David, H. Zacharias, Surf. Sci. 402 (1998) 232.
[172] A. Eichler, J. Hafner, A. Gross, M. Scheffler, to be published.
[173] K. Christmann, Surf. Sci. Rep. 9 (1988) 1.
[174] R.A. Olsen, P.H.T. Philipsen, E.J. Baerends, G.J. Kroes, O.M. Løvvik, J. Chem. Phys. 106 (1997) 9286.
[175] R.A. Olsen, G.J. Kroes, O.M. Løvvik, E.J. Baerends, J. Chem. Phys. 107 (1997) 10652.
[176] G.E. Gdowski, R.H. Stulen, T.E. Felter, J. Vac. Sci. Technol. A 5 (1987) 1103.

[177] F. Besenbacher, I. Chorkendorff, B.S. Clausen, B. Hammer, A.M. Molenbroek, J.K. Nørskov, I. Stensgaard, Science 279 (1998) 1913.
[178] M.L. Burke, R.J. Madix, Surf. Sci. 237 (1990) 1.
[179] G. Comsa, R. David, B.-J. Schumacher, Surf. Sci. 95 (1980) L210.
[180] A. Gross, to be published.
[181] H. Zacharias, private communication; L. Schröter, Ph.D. thesis, Universität Bielefeld, 1991.
[182] K. Sinniah, M.G. Sherman, L.B. Lewis, W.H. Weinberg, J.T. Yates, K.C. Janda, Phys. Rev. Lett. 62 (1989) 567.
[183] U. Höfer, L. Li, T.F. Heinz, Phys. Rev. B 45 (1992) 9485.
[184] M.C. Flowers, N.B.H. Jonathan, Y. Liu, A. Morris, J. Chem. Phys. 99 (1993) 7038.
[185] J.W. Sharp, G. Eres, Surf. Sci. 320 (1994) 169.
[186] M. Liehr, C.M. Greenlief, M. Offenberg, S.R. Kasi, J. Vac. Sci. Technol. A 8 (1990) 2960.
[187] K.W. Kolasinski, W. Nessler, K.-H. Bornscheuer, E. Hasselbrink, J. Chem. Phys. 101 (1994) 7082.
[188] P. Bratu, U. Höfer, Phys. Rev. Lett. 74 (1995) 1625.
[189] P. Bratu, K.L. Kompa, U. Höfer, Chem. Phys. Lett. 251 (1996) 1.
[190] K.W. Kolasinski, W. Nessler, A. de Meijere, E. Hasselbrink, Phys. Rev. Lett. 72 (1994) 1356.
[191] P. Bratu, W. Brenig, A. Gross, M. Hartmann, U. Höfer, P. Kratzer, R. Russ, Phys. Rev. B 54 (1996) 5978.
[192] W. Brenig, A. Gross, U. Höfer, R. Russ, Phys. Status Solidi (a) 159 (1996) 75.
[193] C.J. Wu, I.V. Ionova, E.A. Carter, Surf. Sci. 295 (1993) 64.
[194] Z. Jing, G. Lucovsky, J.L. Whitten, Surf. Sci. 296 (1993) L33.
[195] P. Nachtigall, K.D. Jordan, C. Sosa, J. Chem. Phys. 101 (1994) 8073.
[196] P. Nachtigall, K.D. Jordan, J. Chem. Phys. 102 (1995) 8249.
[197] Z. Jing, J.L. Whitten, J. Chem. Phys. 102 (1995) 3867.
[198] M.R. Radeke, E.A. Carter, Surf. Sci. 355 (1996) L289.
[199] M.R. Radeke, E.A. Carter, Phys. Rev. B 54 (1996) 11803.
[200] M.R. Radeke, E.A. Carter, Phys. Rev. B 55 (1997) 4649.
[201] Z. Jing, J.L. Whitten, Phys. Rev. B 46 (1992) 9544.
[202] J. Dabrowski, M. Scheffler, Appl. Surf. Sci. 56 (1992) 15.
[203] J.E. Northrup, Phys. Rev. B 47 (1993) 10032.
[204] R.A. Wolkow, Phys. Rev. Lett. 68 (1992) 2636.
[205] E.L. Bullock, R. Gunnella, L. Patthey, T. Abukawa, S. Kono, C.R. Natoli, L.S.O. Johansson, Phys. Rev. Lett. 74 (1995) 2756.
[206] A.R. Smith, F.K. Men, K.-J. Chao, C.K. Shih, J. Vac. Sci. Technol. B 14 (1996) 914.
[207] C. Yang, S.Y. Lee, H.C. Kang, J. Chem. Phys. 107 (1997) 3295.
[208] P. Kratzer, B. Hammer, J.K. Nørskov, Chem. Phys. Lett. 229 (1994) 645.
[209] P. Kratzer, B. Hammer, J.K Nørskov, Phys. Rev. B 51 (1996) 13432.
[210] E. Pehlke, M. Scheffler, Phys. Rev. Lett. 74 (1995) 952.
[211] A. Vittadini, A. Selloni, Chem. Phys. Lett. 235 (1995) 334.
[212] S. Pai, D. Doren, J. Chem. Phys. 103 (1995) 1232.
[213] P. Kratzer, R. Russ, W. Brenig, Surf. Sci. 345 (1996) 125.
[214] A.C. Luntz, P. Kratzer, J. Chem. Phys. 104 (1996) 3075.
[215] K.W. Kolasinski, S.F. Shane, R.N. Zare, J. Chem. Phys. 96 (1992) 3995.
[216] Y.-S. Park, J.-Y. Kim, J. Lee, J. Chem. Phys. 98 (1993) 757.
[217] M.C. Flowers, N.B.H. Jonathan, A. Morris, S. Wright, J. Chem. Phys. 108 (1998) 3342.
[218] M.B. Raschke, U. Höfer, Surf. Sci. Lett., submitted; P. Kratzer, E. Pehlke, M. Scheffler, M.B. Raschke, U. Höfer, submitted.
[219] P.L. Silvestrelli, A. Alavi, M. Parrinello, D. Frenkel, Phys. Rev. Lett. 77 (1996) 3149.
[220] L. Gavioli, M.G. Betti, C. Mariani, Phys. Rev. Lett. 77 (1996) 3869.
[221] E.W. Kuipers, A. Vardi, A. Danon, A. Amirav, Phys. Rev. Lett. 66 (1991) 116.
[222] C.T. Rettner, Phys. Rev. Lett. 69 (1992) 383.
[223] C.T. Rettner, D.J. Auerbach, J. Chem. Phys. 104 (1996) 2732.
[224] T.A. Jachimowski, W.H. Weinberg, J. Chem. Phys. 101 (1994) 10997.
[225] W. Widdra, S.I. Yi, R. Maboudian, G.A.D. Briggs, W.H. Weinberg, Phys. Rev. Lett. 74 (1995) 2074.

[226] S.A. Buntin, J. Chem. Phys. 108 (1998) 1601.
[227] G. Schulze, M. Henzler, Surf. Sci. 124 (1983) 336.
[228] S. Wehner, J. Küppers, J. Chem. Phys. 108 (1998) 3353.
[229] P. Kratzer, J. Chem. Phys. 106 (1997) 6752.
[230] J. Harris, B. Kasemo, Surf. Sci. 105 (1981) L281.
[231] B. Jackson, M. Persson, J. Chem. Phys. 96 (1992) 2378.
[232] M. Persson, B. Jackson, J. Chem. Phys. 102 (1995) 1078.
[233] J. Strömquist, L. Bengtsson, M. Persson, B. Hammer, Surf. Sci. 397 (1998) 382.
[234] W. Brenig, D. Menzel (Eds.), Desorption Induced by Electronic Transitions, DIET II, Springer, Berlin, 1985.
[235] F.M. Zimmermann, W. Ho, Surf. Sci. Rep. 22 (1995) 127.
[236] J.W. Gadzuk, Annu. Rev. Phys. Chem. 39 (1988) 395.
[237] P. Saalfrank, Surf. Sci. 390 (1997) 1.
[238] S.M. Harris, S. Holloway, G.R. Darling, J. Chem. Phys. 102 (1995) 8235.
[239] P. Saalfrank, Chem. Phys. 193 (1995) 119.
[240] T. Hertel, M. Wolf, G. Ertl, J. Chem. Phys. 102 (1995) 3414.
[241] K.-H. Bornscheuer, W. Nessler, M. Binetti, E. Hasselbrink, P. Saalfrank, Phys. Rev. Lett. 78 (1997) 1174.
[242] T. Klüner, H.-J. Freund, J. Freitag, V. Staemmler, J. Chem. Phys. 104 (1996) 10030.
[243] H. Kuhlenbeck, G. Odörfer, R. Jaeger, G. Illing, M. Menges, Th. Mull, H.-J. Freund, M. Pöhlchen, V. Staemmler, S. Witzel, C. Scharfschwerdt, K. Wennemann, T. Liedte, M. Neumann, Phys. Rev. B 43 (1991) 1969.
[244] P.R. Antoniewicz, Phys. Rev. B 21 (1980) 3811.
[245] Th. Mull, B. Baumeister, M. Menges, H.-J. Freund, D. Weide, C. Fischer, P. Andresen, J. Chem. Phys. 96 (1992) 7108.
[246] W. Brenig, R. Brako, M.F. Hilf, Z. Phys. Chem. 197 (1996) 237.